

RIVM Report 728001012

**Assessment of major uncertainties in calculating  
regional contributions to climate change**

Michel den Elzen, Michiel Schaeffer

September 2000

This research has been conducted on behalf and for the account of the National Institute of Public Health and the Environment (RIVM), the Ministry of Housing, Spatial Planning and Environment (VROM) within the framework of project 728001, and the Dutch National Research Programme on Global Air Pollution and Climate Change (NRP) (project 954285).

Department for Environmental Information Systems (CIM) and  
Department for Environmental Assessment (MNV)  
National Institute of Public Health and the Environment (RIVM)  
P.O. Box 1, 3720 BA Bilthoven  
The Netherlands  
Telephone : +31 30 2743584  
Fax: : +31 30 2744427  
E-mail : [Michel.den.Elzen@rivm.nl](mailto:Michel.den.Elzen@rivm.nl)/ [image-info@rivm.nl](mailto:image-info@rivm.nl)

---

## MAILING LIST

1. Directeur Lucht en Energie van het Directoraat-Generaal voor Milieubeheer
2. Plv. Directeur-Generaal Milieubeheer, dr. ir. B.C.J. Zoeteman
3. Hoofd Klimaatverandering DGM-LE, T. Fogelberg
4. Plv. Hoofd Klimaatverandering DGM-LE, dr. L.A. Meyer
- 5-10. Secretariaat NOP Mondiale Luchtverontreiniging en Klimaatverandering
11. Ir. drs. R.B.J.C. van Noort
12. Prof. ir. N.D. van Egmond
13. Ir. F. Langeweg
14. Drs. A.H. Bakema, CIM
15. Drs. J.A. Bakkes, MNV
16. Ir. R. van den Berg, LBG
17. Drs. M. Berk, MNV
18. Drs. A.H.W. Beusen, CIM
19. Drs. J.C. Bollen, MNV
20. Drs. S. Both, MNV
21. Dr. A.A. Bouwman, LBG
22. Drs. L.C. Braat, CIM
23. Ir. A.H.M. Bresser, LWD
24. Drs. B. Eickhout, MNV
25. Drs. A. van der Giessen, LBG
26. Drs. C. Graveland, MNV
27. Drs. H.A.R.M. Heiligenberg, CIM
28. Prof. Dr. J.P. Hettelingh, MNV
29. Drs. H.B.M. Hildering, MNV
30. Dr. J.A. Hoekstra, LAE
31. Ir. N.J.P. Hoogervorts, LAE
32. Dr. M.A. Janssen
33. Dr. L.H.J.M. Janssen, LLO
34. Ir. G.J.J. Kreileman, CIM
35. Dr. M.A.J. Kuijpers-Linde, LAE
36. Dr. R. Leemans, MNV
37. Dr. D. van Lith, LLO
38. Drs. R.J.M. Maas, MNV
39. Dr. B. Metz, MNV
40. Drs. J. Minnen, MNV
41. C.H. Oostenrijk, CIM
42. Dr. J.H. Pan, MNV
43. Drs. J.P.M. Ros, LAE
44. Dr. R.J. Swart, LLO
45. Dr. H.J.M. de Vries, MNV
46. Drs. J.W. van Woerden, CIM
47. Mr. Y. de Boer, VROM, Directie Internationale Milieuzaken, Den Haag
48. Mr. W. Hare, Greenpeace International, Amsterdam
49. Prof. Dr. A.A.M. Holtslag, Wageningen University, Wageningen
50. Mr. L. Meyer, VROM, Directoraat-Generaal Milieu Beheer, Den Haag
51. Mr. H. Nieuwehuizen, VROM, Directoraat-Generaal Milieu Beheer, Den Haag
52. Ms. M. I. Oosterman, DGIS, Min. BuZa, Den Haag
53. Dr. R. Ball, U.S. Department of Energy, Washington, USA
54. Dr. S. Barrel, Bureau of Meteorology, Australia
55. Mr. K. Dixon, Geophysical Fluid Dynamics Laboratory, Princeton, USA
56. Mr. H. Hengeveld, Environment Canada, Canada

- 57. Mr. G. Hooss, MPI Meteorology, Hamburg, Germany
- 58. Dr. C. Mitchel, CSIRO, Australia
- 59. Dr. J.D.G. Miquez, MTU, Brazil
- 60. Mr. N. Paciornik, MTU, Brazil
- 61. Dr. C.A. Senior, Hadley Centre for Climate Prediction and Research, U.K. Met Office., UK
- 62. Dr. D. Viner, University of East Anglia, Norwich, UK
- 63. Dr. R. Voss, MPI Meteorology, Hamburg, Germany
- 64. Dr. I.G. Watterson, CSIRO, Australia
- 65-100 Authors
- 101 Hoofd Bureau Voorlichting en Public Relations
- 102 Depot van Nederlandse publicaties en Nederlandse bibliografie
- 103 Bibliotheek RIVM
- 104 Bibliotheek MNV
- 105 Bureau Rapportenregistratie
- 106-150 Bureau Rapportenbeheer

---

## ACKNOWLEDGEMENTS

This study took place at the National Institute of Public Health and the Environment (RIVM) with the support of the National Research Programme on Global Air Pollution and Climate Change (NRP), the Dutch Ministry of Housing, Spatial Planning and the Environment (VROM) and RIVM under projects MAP-728001 and MAP- 490200, and the NRP-project-954285. We like to thank the NRP, VROM and RIVM for their continued support of this study. Special thanks are due to our advisory committee consisting of Dr. Leo Meyer (VROM) and Ms. Maresa Oosterman (KNMI), who have provided us with critical and useful comments.

We owe a vote of thanks to the participants of the Expert meeting on the Brazilian Proposal in Cachoeira (Brazil, May, 1999). In particular, we would like to thank Luiz Gylvan Meira Filho and Jose Domingos Gonzales Miquez (Brazil), Ian Enting and Chris Mitchel (Australia), Henry Hengeveld (Canada), Geoff Jenkins (United Kingdom), and Daniel Lashof and Raymond Prince (USA), for their contributions.

We appreciated very much the remarks and advise of the climate scientists who kindly provided us with their model data. We would especially like to thank Keith Dixon (GFDL, USA), Catherine Senior (Hadley Centre, UK), Ron Stouffer (GFDL, USA), David Viner (UEA, UK), Reinhard Voss (MPI Meteorology, Germany) and Ian Watterson (CSIRO, Australia).

Finally, we are grateful to the whole IMAGE team and other colleagues at the RIVM, in particular, Marcel Berk, Rik Leemans and Bert Metz. Special thanks go to Ruth de Wijs for correcting the English text.

This report is a modified version of our manuscript “Evaluating major scientific uncertainties of the Brazilian Proposal for emission reduction burden sharing”, submitted to *climatic change* in july 2000.



## ABSTRACT

During the negotiations on the Kyoto Protocol, Brazil proposed a methodology to link the relative contribution of Annex-I Parties to emission reductions with the relative contributions of Parties to the global-mean temperature increase. The proposal was not adopted during the negotiations, but referred to the Subsidiary Body for Scientific and Technological Advice for consideration of its methodological aspects. In this report we analyze the impact of model uncertainties and methodological choices on the regionally attributed global-mean temperature increase. A climate assessment model was developed, which calculates changes in greenhouse gas concentrations, global-mean temperature and sea-level rise attributable to individual regions. The analysis shows the impact of the different choices in methodological aspects to be as important as the impact of model uncertainties on a region's contribution to present and future global temperature increase. Choices may be the inclusion of the anthropogenic non-CO<sub>2</sub> greenhouse gas emissions and/or the CO<sub>2</sub> emissions associated with land-use changes. When responsibility to global temperature change is attributed to all emitting parties, the impacts of modeling uncertainties and methodological choices are considerable. However, if relative contributions are calculated only within the group of Annex-I countries, the results are remarkably insensitive to the uncertainty aspects considered here.

*Keywords: Model uncertainty, Climate change, Brazilian proposal, Climate assessment model, Burden sharing and FAIR model.*

Note: This report has also been submitted as an article for the journal Climatic change.

---

## SAMENVATTING

Gedurende de onderhandelingen over het Kyoto Protocol, werd door Brazilië het zogenaamde Braziliaanse voorstel ingediend. Dit voorstel omvat o.a. een methodiek om de relative bijdrage van de geïndustrialiseerde landen (Annex I) aan de emissiereducties te baseren op hun relatieve bijdrage aan de mondiaal gemiddelde temperatuurstijging die inmiddels is opgetreden. Hoewel het Braziliaanse voorstel niet werd opgenomen in het Kyoto Protocol, besloot de Conferentie van Partijen bij het klimaatverdrag (COP3) in Kyoto het voorstel door te verwijzen naar SBSTA ('Subsidiary Body on Scientific and Technical Advice') van de UNFCCC ('United Nations Framework Convention on Climate Change') om daar de wetenschappelijke en methodologische aspecten van het voorstel nader te bestuderen.

In dit rapport presenteren we een analyse van het effect van modelonzekerheden en methodologische aspecten op de individuele regionale bijdrage aan de mondiale gemiddelde temperatuurstijging. Voor dit doeleinde is het klimaatmodel meta-IMAGE 2.1 gebruikt. Meta-IMAGE berekent de regionale bijdrage aan de klimaatsindicatoren in de oorzaak-effect keten van het klimaatprobleem, i.e. de antropogene CO<sub>2</sub>-emissies, de stijging van de atmosferische CO<sub>2</sub>-concentratie, en de mondiale temperatuurstijging en zeespiegelstijging. De analyse toont aan dat het effect op de modeluitkomsten van modelonzekerheden in dezelfde orde van grootte ligt als het effect van methodologische aspecten. Methodologische keuzes zijn onder andere het meenemen van de antropogene emissies van alle broeikasgassen en/of de emissies ten gevolge van landgebruikveranderingen.

Een mondiale toepassing van het Braziliaanse voorstel, i.e. het gebruik van de bijdrage aan mondiale temperatuurstijging als criterium voor lastenverdeling, impliceert een groot effect van modelonzekerheden en methodologische keuzes op de regionale bijdrage aan de mondiale gemiddelde temperatuurstijging. Een soortgelijke berekening van de regionale bijdragen binnen de Annex I groep, blijkt daarentegen veel minder gevoelig te zijn voor deze modelonzekerheden en methodologische aspecten.

---

## CONTENTS

<b>1 INTRODUCTION .....</b>	<b>11</b>
<b>2 MODELING APPROACH FOR ATTRIBUTING ANTHROPOGENIC CLIMATE CHANGE ....</b>	<b>15</b>
2.1 FROM EMISSIONS TO CONCENTRATION .....	15
2.2 FROM CONCENTRATION TO RADIATIVE FORCING.....	17
2.3 FROM RADIATIVE FORCING TO TEMPERATURE INCREASE.....	18
<b>3 MODEL ANALYSIS OF A REGION'S CONTRIBUTION TO GLOBAL WARMING: MODEL UNCERTAINTIES.....</b>	<b>23</b>
3.1 INTRODUCTION .....	23
3.2 INPUT DATA .....	23
3.3 VARIOUS BALANCING APPROACHES FOR THE PAST CARBON BUDGET .....	24
3.4 USING TEMPERATURE RESPONSE FUNCTIONS OF VARIOUS AOGCMS .....	27
3.5 OVERALL UNCERTAINTIES OF GLOBAL CARBON CYCLE AND CLIMATE MODELS.....	29
<b>4 MODEL ANALYSIS OF A REGION'S CONTRIBUTION TO GLOBAL WARMING: METHODOLOGICAL CHOICES.....</b>	<b>31</b>
4.1 INTRODUCTION .....	31
4.2 INCLUSION OF VARIOUS ANTHROPOGENIC EMISSIONS SOURCES OF GREENHOUSE GASES .....	31
4.3 NON-LINEAR APPROACH TO CALCULATE CONTRIBUTIONS TO RADIATIVE FORCING .....	32
4.4 OTHER EMISSIONS SCENARIOS.....	32
4.5 OTHER CLIMATE INDICATORS: RATE OF TEMPERATURE INCREASE AND SEA-LEVEL RISE.....	33
4.6 RESPONSIBILITY ATTRIBUTED TO ANNEX-I REGIONS ONLY .....	33
<b>5 CONCLUSIONS.....</b>	<b>35</b>
<b>REFERENCES .....</b>	<b>37</b>
<b>Appendix.....</b>	<b>40</b>



## 1 Introduction

One of the key policy issues in the evolution of the United Nations Framework Convention on Climate Change (UNFCCC) is the future involvement of “developing country” Parties (non-Annex I) in reducing global greenhouse gas emissions. While emissions from these developing countries currently constitute a minor proportion of global greenhouse gas emissions, they are expected to outgrow those of the industrialized countries (Annex I) within several decades. However, even during the negotiations on the UNFCCC in 1992, developing countries stressed that given their historical emissions, the industrialized countries should bear the primary responsibility for the climate problem and should be the first to act. This was formally recognized in the UNFCCC (1992) which states that developed and developing countries have “common but differentiated responsibilities”. It was re-acknowledged in the so-called Berlin Mandate (1995), which permitted additional commitments for industrialized countries only.

In this context, the proposal made by Brazil during the negotiations for the Kyoto Protocol (UNFCCC, 1998) is interesting, since it proposes a methodology for linking an Annex I country’s contribution to emission control to its contribution to global warming (UNFCCC, 1997). In this way, historical emissions are included in sharing the burden of emission control. Although the proposal was initially developed to help discussions on burden sharing among Annex I countries, it can also be used as a framework for discussions between Annex I and non-Annex I countries on future participation of all countries in emission reductions. In essence, it applies the “polluter pays” principle to climate change. During the Kyoto negotiations the Brazilian Proposal was not adopted, but did receive support, especially from developing countries. To keep this concept on the agenda, the Third Conference of the Parties (COP-3) decided to ask the Subsidiary Body on Scientific and Technical Advice (SBSTA) of the UNFCCC to further study the methodological and scientific aspects of the proposal.

As a starting point, the Brazilian proposal concentrated on contributions of emissions to global-mean surface-air temperature increase (henceforth known simply as “temperature increase”). During the initial discussion at SBSTA-8 in February 1998, some participants suggested considering the contribution of emissions to the rate of temperature increase and sea-level rise as well. At that meeting, Brazil offered to organize a related expert meeting to evaluate the methodological and scientific aspects of the Brazilian Proposal. At COP-4 in Buenos Aires in November 1998, the SBSTA-9 noted the information provided by Brazil on recent scientific activities, including a revision of the methodology (Filho and Miquez, 1998), and invited Brazil to inform the SBSTA at the tenth session in Bonn in June 1999 on the results of its expert meeting. Since COP-3 (1997) several groups in various countries, including China, Canada, France, the United States of America, Australia and the Netherlands have assessed the Brazilian proposal and its analysis and found similar deficiencies both in the original proposal and its analysis (e.g. Enting, 1998; Berk and Den Elzen, 1998). Most of these deficiencies were adequately addressed in the revised Brazilian methodology (see Den Elzen et al. (1999) for an evaluation of the revised methodology). During COP-4 the Dutch National Institute of Public Health and the Environment (RIVM) organized an informal expert meeting in consultation with Brazil to exchange information and explore relevant issues for the international expert meeting. This international Expert Meeting was held in May 1999 in Brazil, where it was concluded that the scientific and technical basis for putting the Brazilian proposal into operation would be sufficient (Den Elzen, 1999). However, there are still some related scientific aspects that need to be more thoroughly assessed and understood like, for example, the issue of the non-linearity of radiative forcing, which Enting (1998) first raised. During the discussions at SBSTA-10 (Bonn, June 1999), it was therefore decided to put the issue of attributing responsibility to climate change on the agenda of the IPCC.

In our view, the central question in this issue is: Does the present state of knowledge permit evaluating individual parties' contribution to the climate change problem within an acceptable uncertainty range? Of course, we will leave it to the reader to decide what uncertainty is "acceptable". Our present analysis concentrates on several important sources of uncertainty that can be quantified with the present modeling tools. More specifically, we will evaluate uncertainties in carbon-cycle and climate modeling, as well as specific methodological aspects as discussed in the Expert Meeting. We will assess their impacts on calculations of regional contribution to temperature increase and other climate indicators, such as sea-level rise and rate of temperature increase. A simple climate assessment model was developed for this purpose; it calculates the concentrations of greenhouse gases, radiative forcing, temperature and sea-level rise. To complement this model, we have developed a climate "attribution" module to calculate the regional contributions to various categories of emissions, concentrations of greenhouse gases, and temperature and sea-level rise. The thirteen world regions considered are: Canada, USA, Latin America, Africa, OECD-Europe, Eastern Europe, CIS, Middle East, India and South Asia, China and centrally planned Asia, West Asia, Oceania and Japan. The methodology can be extended to country level, as already done for a selected group of eleven countries (i.e. Australia, England, Germany, Japan, The Netherlands, USA, Brazil, China, India, Mexico and South Africa in Den Elzen et al. (1999)). The model projections in the analysis presented here will only focus on the global, Annex I/non-Annex I and regional levels.

This study follows the Brazilian Proposal in focusing on the regional anthropogenic emissions of the major greenhouse gases regulated in the Kyoto Protocol (i.e. carbon dioxide (CO<sub>2</sub>), methane (CH<sub>4</sub>) and nitrous dioxide (N<sub>2</sub>O)). Here and in the Brazilian Proposal, the term "anthropogenic emissions" is used for the net anthropogenic emissions of greenhouse gases or the difference between anthropogenic emissions by sources and direct anthropogenic removals by sinks of greenhouse gases. The other greenhouse gases included in the Kyoto Protocol i.e. hydrofluorocarbons (HFCs), perfluorocarbons (PFCs) and sulphur hexafluoride (SF<sub>6</sub>), are not taken into account since no regional emission data are available. The anthropogenic emissions of these gases, and the other halocarbons, i.e. CFCs, methyl chloroform, carbon tetrachloride, halons and HCFCs (Montreal Protocol), ozone precursors and SO<sub>2</sub> (Clean Air protocols), as well as the natural emissions of all greenhouse gases, are considered at the global level only.

Figure 1 depicts the climate assessment model, as used for the model analysis. At the core of the simple climate assessment model is the integrated simple climate model, meta-IMAGE 2.1 (henceforth to be referred to as meta-IMAGE) (Den Elzen, 1998; Den Elzen et al., 1997). Meta-IMAGE is a simplified version of the more complex climate assessment model IMAGE 2. The latter aims at a more thorough description of the complex, long-term dynamics of the biosphere-climate system at a geographically explicit level (0.5° x 0.5° latitude-longitude grid) (Alcamo, 1994; Alcamo et al., 1996; 1998). Meta-IMAGE is a more flexible, transparent and interactive simulation tool that adequately reproduces the IMAGE-2.1 projections of global atmospheric concentrations of greenhouse gases, along with the temperature increase and sea-level rise for the various IMAGE 2.1 emissions scenarios. Meta-IMAGE consists of an integration of a global carbon cycle model (Den Elzen et al., 1997), an atmospheric chemistry model (Krol and Van der Woerd, 1994), and a climate model (upwelling-diffusion energy balance box model of Wigley and Schlesinger (1985) and Wigley and Raper (1992)). This core model has been supplemented with the following new elements: (i) the revised Brazilian model (Filho and Miquez, 1998), (ii) a climate "attribution" module and (iii) global temperature impulse response functions (IRFs, e.g. Hasselmann et al., 1993) based on simulation experiments with various Atmosphere-Ocean General Circulation Models (AOGCMs) for alternative temperature increase calculations. We have also implemented the global carbon cycle model of the MAGICC (Wigley, 1993) and Bern model (Joos et al., 1996) solely for the purpose of alternative CO<sub>2</sub> concentration calculations in the model analysis presented here. This climate assessment model forms an integral part of our overall FAIR model (Framework to Assess

International Regimes for burden sharing), which was developed to explore options for international burden sharing, including the Brazilian approach (Den Elzen et al., 1999).

This report is built up as follows. Chapter 2 briefly describes the background and modeling approaches used for calculating the concentrations, radiative forcing, temperature and sea-level rise projections. The model analysis on the uncertainties (Chapter 3) first assesses the impact of various carbon balancing mechanisms on regional contribution to global temperature increase. This involves balancing the past carbon budget within the range of IPCC estimates for the terrestrial and oceanic uptake, and for CO<sub>2</sub> emissions from land-use changes. In addition, alternative carbon cycle model calculations are performed. Subsequently, we will assess the role of uncertainties in climate response to radiative forcing, i.e. different global temperature response functions. Results of both exercises will be combined to assess overall uncertainties. Chapter 4 assesses the impact of methodological choices, i.e. alternative climate indicators (rate of temperature increase and sea-level rise), Enting's (1998) methodology of attributing non-linear radiative forcing, including other than fossil CO<sub>2</sub> emissions, such as CO<sub>2</sub> emissions from land-use changes and anthropogenic CH<sub>4</sub> and N<sub>2</sub>O emissions, and the impact of the composition of the group of regions among which responsibility is shared (world vs. Annex-I). Chapter 5 concludes our evaluation.

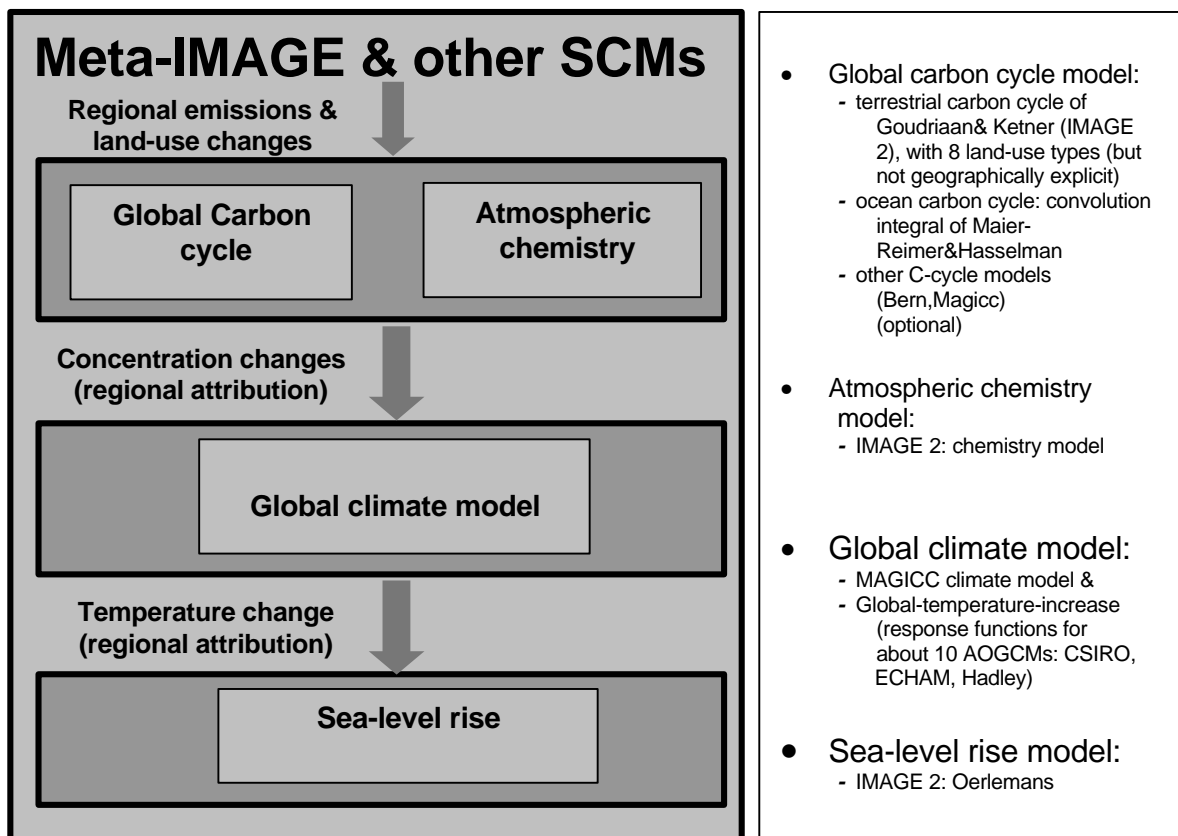


Figure 1. The climate assessment model of FAIR as used for the model analysis.



## 2 Modeling approach for attributing anthropogenic climate change

### 2.1 From emissions to concentration

#### *Global concentrations of greenhouse gases*

The emissions of a greenhouse gas and its subsequent removal from the atmosphere determine the concentration. The lifetime of a greenhouse gas indicates the efficiency of the removal process and is a measure of the time that passes before an emission pulse is removed from the atmosphere. For nitrous dioxide (N<sub>2</sub>O) and the halocarbons, the rate of removal is linearly dependent on the concentration of the compound, and is derived by multiplying the concentration by a constant lifetime factor, as adopted in most current IPCC SCMs (Harvey et al., 1997). The rate of change for the concentration is then expressed as:

$$\frac{dr_g}{dt} = cv_g E_g - r_g / t_g \quad (1)$$

where  $r_g$  is the atmospheric concentration of greenhouse gas  $g$ ,  $E_g$  the anthropogenic emissions,  $t_g$  the atmospheric exponential decay time or lifetime (yr) and  $cv_g$  a mass-to-concentration conversion factor. For meta-IMAGE, the lifetime of the HCFCs, HFCs and CH<sub>3</sub>CCl<sub>3</sub> is also a function of the tropospheric OH concentration. For the major greenhouse gases CO<sub>2</sub> and CH<sub>4</sub>, the SCMs differ with respect to the modeling of the translation between the emissions and concentrations; this will be described in the overview below.

*Carbon dioxide* - The carbon cycle is an integral part of the climate system, governing the changes of atmospheric CO<sub>2</sub> concentration in response to the anthropogenic CO<sub>2</sub> emission from fossil-fuel burning and land-use changes. This entanglement of climate system and carbon cycle gives rise to a range of uncertainties, which is reflected by the wide variety of existing modeling approaches. Global-mean carbon-cycle models consist of a well-mixed atmosphere linked to oceanic and terrestrial biospheric compartments. These models, driven by the anthropogenic CO<sub>2</sub> emissions, calculate the terrestrial and oceanic sinks and the resulting atmospheric CO<sub>2</sub> build-up.

The oceanic component of simple carbon-cycle models can be formulated as an upwelling-diffusion model (Siegenthaler and Joos, 1992), or be represented by a mathematical function (known as a convolution integral), which can be attuned to closely replicate the behavior of more complex oceanic models (Harvey, 1989). The carbon-cycle models of MAGICC (Wigley, 1991), meta-IMAGE (Den Elzen, 1998) and the revised Brazilian model use the latter approach. The Bern carbon-cycle model (Joos et al., 1996) uses a more accurate representation of a convolution integral, i.e. an ocean mixed-layer pulse response function (surface deep-ocean mixing) in combination with an equation describing air-sea exchange.

The terrestrial component in carbon cycle models is vertically differentiated into carbon reservoirs (Harvey, 1989), such as two living biomass boxes, a detritus and a soil box as in MAGICC (Wigley, 1993). In meta-IMAGE, the four terrestrial carbon boxes model (biomass, litter/detritus, humus, soil) is further differentiated horizontally into eight land-use types, i.e. forests, grasslands, agriculture and other land for the developing and industrialized world (Elzen, 1998). This allows us to analyze the effect of land-use changes such as deforestation on the global carbon cycle. The Bern model uses a decay-response function describing the carbon cycling in the terrestrial reservoirs in combination with an equation describing the net primary production. The revised Brazilian model ignores the terrestrial carbon cycle, and only focuses on the slow oceanic carbon dynamics.

To obtain a balanced past carbon budget of anthropogenic CO<sub>2</sub> emission in these carbon-cycle models, and therefore a good fit between the historically observed and simulated atmospheric

CO<sub>2</sub> concentration, it is essential to introduce terrestrial sinks (Schimel et al., 1995) in addition to oceanic sinks. In the MAGICC model, the past carbon budget is solely balanced by the CO<sub>2</sub> fertilization effect on the terrestrial biosphere, whereas in meta-IMAGE, temperature feedbacks on net primary production and soil respiration are also present. Although the N fertilization feedback was included in the earlier version of the meta-IMAGE model (Den Elzen et al., 1997), it is now excluded due to the need for it to be consistent with IMAGE 2.1 (Den Elzen, 1998), as well as with the new scientific insights of Nadelhoffer et al. (1999). Based on recent N-15 tracer studies, Nadelhoffer et al. concluded that it is unclear whether elevated nitrogen deposition is the primary cause of C sequestration in northern forests. To evaluate the climate-change related terrestrial feedbacks on a process base and with the necessary geographical explicitness, a more complex model like the IMAGE 2.1 model should be used (Alcamo et al., 1996; 1998). Here we use the insights gained from experiments with the IMAGE 2.1 model to find a parameterization of the CO<sub>2</sub> fertilization and temperature feedbacks in meta-IMAGE. The modeling of these feedback mechanisms affects the future CO<sub>2</sub> concentration projections. Various model parameterizations of these feedbacks, each leading to a balanced past carbon budget in carbon cycle models, can be shown to result in a wide range of future CO<sub>2</sub> concentration projections (Schimel et al., 1995). This is caused by the carbon balancing procedure's influence on the relative amount of carbon uptake by fast and slow overturning reservoirs.

A disadvantage of a simple model framework is the inability to capture potentially important non-linear or "extreme" events. However, information can be drawn from more complex models, which can be used in a simpler model. An example is provided here by evaluating an additional large source of uncertainty. Preliminary results of experiments using global dynamic vegetation models suggest that the influence of climatic change on (land) vegetation in some Dynamic Global Vegetation Models might result in a shift of its functioning as a CO<sub>2</sub> sink to a source in the second half of the next century (Cramer et al., in press). As an extreme example, we will apply an idealized representation of the results of one such model (White et al., 1999). The projected large decrease in sink size for this model might be explained by the large forest fraction in the simulation of present-day land cover, making the model relatively sensitive to drought. To reflect this model's results in an idealized experiment, we will linearly decrease carbon uptake by the terrestrial vegetation in meta-IMAGE (as represented by Net Ecosystem Productivity [NEP]) from the value it has in 2050 to 0 in 2100 (see section 3.2).

*Methane* - The chemical removal rate and atmospheric lifetime of CH<sub>4</sub> depend on the concentration of CH<sub>4</sub> itself, and are also affected by the concentrations and emissions of the gases NO<sub>x</sub>, CO and VOCs, and the tropospheric concentration of OH. The current lifetime is about nine years (Harvey et al., 1997). In addition to removal by chemical reactions in the atmosphere, CH<sub>4</sub> is also absorbed by soils, with a specific time constant of 150 years. In meta-IMAGE the CH<sub>4</sub> lifetime is a function of the transport losses to both stratosphere and biosphere, and the average atmospheric residence time. This function depends on the OH concentration (Krol and Van der Woerd, 1994). In MAGICC this residence time depends only on the emissions of CH<sub>4</sub> itself (Osborn and Wigley, 1994). In the revised Brazilian model, a constant CH<sub>4</sub> lifetime is used.

#### *Concentrations attributed*

Calculations of regional contributions to concentration increases can be done in a straightforward manner using the mass balance equation (1) with regional anthropogenic emissions and a regional sink term. This is calculated as:  $\mathbf{r}_{g,r}(t)/\mathbf{t}_g(t)$ , in which  $\mathbf{r}_{g,r}(t)$  is the regional atmospheric concentration of greenhouse gas  $g$  at time  $t$ . As mentioned above, only the major greenhouse gases, i.e. CO<sub>2</sub>, CH<sub>4</sub> and N<sub>2</sub>O, are accounted for in calculating contributions of regions, whereas the influence of emissions of the other greenhouse gases and aerosols are considered at global level.

## 2.2 From concentration to radiative forcing

### *Global radiative forcing*

Increased concentrations of greenhouse gases in the atmosphere lead to a change in radiative forcing, a measure of the extra energy input to the surface-troposphere system. As the concentration of a greenhouse gas increases, this dependence of forcing on concentration will gradually "saturate" in certain absorption bands. An additional unit increase of concentration will gradually have a relatively smaller impact on radiative forcing. At present-day concentrations, the saturation effect is greatest for CO<sub>2</sub> and somewhat less for CH<sub>4</sub> and N<sub>2</sub>O. Additionally, some greenhouse gases absorb radiation in each other's frequency domains. This "overlap effect" is especially relevant for CH<sub>4</sub> and N<sub>2</sub>O. Increases in CH<sub>4</sub> concentration decrease the efficiency of N<sub>2</sub>O absorption and vice versa. The present SCMs such as MAGICC and meta-IMAGE use the global radiative forcing dependencies of the IPCC (Harvey et al., 1997), including the major saturation and overlap effects. In our present study, we will not include uncertainties in radiative forcing, as these are considered relatively low for the major greenhouse gases included here (IPCC, 1995).

### *Radiative forcing attributed*

Calculating regional contributions to global radiative forcing by a greenhouse gas is more complicated than contributions to concentration increases. Due to the saturation effect, the radiative forcing of each additional unit of concentration from the "early emitters" (no saturation of CO<sub>2</sub> absorption) is larger than the radiative forcing of an additional unit from the "later emitters" (partial saturation of CO<sub>2</sub> absorption). When more regions start to contribute, a decision will have to be made on how to divide the "benefit" of the overlap or saturation, otherwise the sum of the partial effects would exceed the whole radiative effect (Enting, 1998). The resulting regional radiative forcing depends on the methodology followed. There are two possibilities: the radiative forcing ( $Q_g$  in W·m<sup>-2</sup>) may be calculated in proportion to (i) attributed concentrations of a greenhouse gas, or (ii) the changes in attributed concentrations. The methodology of (ii), the non-linear approach to calculate contributions to radiative forcing, is described in Enting (1998):

$$Q_g(r) = \int \frac{dq_g}{dr_g} \frac{dr_g(r)}{dt} dt \quad (2)$$

where  $q_g(\mathbf{r}_g)$  is the radiative forcing function of greenhouse gas,  $g$ , depending on its concentration,  $\mathbf{r}_g$ . Each component accounts for the importance of each year's radiative effect, depending on the total contributions from all regions over previous years (through the use of the time-dependent factor  $dq_g/dr_g$ ). Similar to calculating contributions to concentration increases, only CO<sub>2</sub>, CH<sub>4</sub> and N<sub>2</sub>O are accounted for here. This implies that the total radiative forcing consists of the sum of radiative forcings caused by the CO<sub>2</sub>, CH<sub>4</sub> and N<sub>2</sub>O emissions for individual regions, and the overall radiative forcing caused by the global emissions of the other greenhouse gases and aerosols (a separate category).

The first methodology ignores the partial saturation effect and considers equal radiative effects of the "early emitters" and the "late emitters", whereas the second includes this partial saturation effect, implying a larger radiative effect of the "early emitters" (Annex I regions). In this report the first methodology has been adopted for the further base calculations. In a later sensitivity analysis we will assess the impact of the second methodology on a region's contribution to anthropogenic climate change.

### 2.3 From radiative forcing to temperature increase

#### *Global mean surface-air temperature increase*

The large heat capacity of the oceans plays an important role in the time-dependent response of the climate system to external forcing. Transport of heat to the deep ocean layers effectively slows down the surface-air temperature response over ocean and land surfaces, as well as in the atmosphere. If the time horizon of a climate change analysis only extends over a few years or decades, the response is, however, dominated by the upper ocean surface layer, reaching relatively rapid adjustment within a few decades. Still, a significant part, roughly 50 percent, of the final global warming will manifest itself decades to centuries later. The delay caused by penetration of heat to the deeper ocean layers is also what causes sea-level rise to continue long after stabilization of greenhouse gas concentrations (Wigley and Raper, 1993). The balance between the rapid and slow adjustment terms is a source of uncertainty, as it depends on non-linear processes like stratification of the upper ocean layers.

The climate sensitivity is another important source of uncertainty in climate response to external forcing. We will use the IPCC (1995) definition, the long-term (equilibrium) annual and global-mean surface-air temperature increase for a doubling CO<sub>2</sub> concentration, denoted by  $\Delta T_{2\times}$ . The climate sensitivity is an outcome of all geophysical feedback mechanisms and their associated uncertainties. The most important source of uncertainty is the hydrological cycle, in particular, clouds and their interaction with radiative processes. IPCC (1995) has estimated the climate sensitivity to lie within the range of 1.5 to 4.5 °C, with a “best-guess” value of 2.5 °C.

Physically, the most rigorous way to analyze climate system response to anthropogenic forcing is provided by “state-of-the-art” AOGCMs. Because they are computationally expensive, these 3-dimensional climate models are difficult to apply in multiple-scenario studies, uncertainty assessments and analysis of feedbacks. In such studies, generally simpler models are applied (e.g. Harvey et al., 1997). As a reference case in our calculations, we will use the upwelling-diffusion box climate model originally described in Wigley and Schlesinger (1985) and updated in Wigley and Raper (1992), as implemented in meta-IMAGE. Our model version uses a default climate sensitivity of  $\Delta T_2 = 2.35$  °C to match IMAGE 2.1 results. For alternative calculations of temperature response, we will derive parameters from a range of AOGCMs to be used in Impulse Response Functions (IRFs). As explained in Hasselmann et al. (1993), IRFs form a simple tool for mathematically describing (“mimic”) transient climate model response to external forcing. A two-term IRF model used here (as in Hasselmann et al., 1993) is based on the following convolution integral, relating temperature response  $\Delta T$  to time-dependent external forcing  $Q(t)$ :

$$\Delta T(t) = \frac{\Delta T_{2\times}}{Q_{2\times}} \int_{t_0}^t Q(t') \left[ \sum_{s=1}^2 l_s (1/t_s) e^{-(t-t')/t_s} \right] dt' \quad (3)$$

where  $Q_{2\times}$  is the radiative forcing for a doubling of CO<sub>2</sub> and  $l_s$  the amplitude of the 1<sup>st</sup> or 2<sup>nd</sup> component with exponential adjustment time constant  $t_s$ , while  $l_1 + l_2 = 1$ .  $\Delta T_2/Q_{2\times}$  equals the climate sensitivity parameter  $I$  (Cess et al., 1989). In an alternative formulation, we can define  $C = I/I$ , and characterize  $C$  as the *effective* heat capacity of the climate system, including climate response feedbacks. The IRF model is mathematically equivalent to a (multi-)box energy balance climate model. Note that in the IRF description these boxes respond independently to the forcing. This makes it impossible to readily link the different IRF terms to specific elements in the physical climate system, like mixed layer and deeper ocean (Hooss et al., 1999). Because we have not found elaborate comparisons of IRF “performance” for a range of AOGCMs in the literature, we will discuss this approach and the problems we encountered below.

Results from a long HadCM2 AOGCM stabilization run (Senior and Mitchell, submitted to *J. Clim.*) suggest that climate sensitivity crucially depends on the state of the climate system. The climate sensitivity in this AOGCM experiment changes from about 2.6 °C over the first 200 years to

3.8 °C after 900 years. Using IRFs with a constant climate sensitivity, as was done here, does not reflect such a model's behavior. Note that a higher sensitivity to radiative forcing later on in the experiment suggests a potentially important "reversed saturation" effect (as opposed to the saturation of radiative forcing, resulting in steadily decreasing sensitivity). In contrast, another study (Watterson, 2000) suggests a steadily increasing effective heat capacity of the climate system. Because of the inverse proportionality of  $DT_2$  and  $C$  as defined here, the sign of the effect found is opposite, resulting in a weaker response to forcing later on in the experiment.

Both studies suggest that a simple model, mimicking AOGCM response, performs better when either climate sensitivity or heat capacity is made time-dependent. In this paper, we have used a constant  $DT_2$  and simply calculated the best fit over a multi-century period of each model's results. For HadCM2, we calculated over this period an average value of 3 °C of the diagnosed climate sensitivity from Senior and Mitchell (submitted). For the other models, we will use the climate sensitivity from the literature. We applied least-square fitting to determine values for the constants  $l_s$  and  $t_s$ , as presented in Table 1; this allows the IRF model to closely mimic the temperature response in a specific AOGCM climate change experiment.

We also included experiments with the simpler climate model of IMAGE 2.1 (Haan et al., 1994). In these experiments, we used two different values for the vertical diffusion coefficient in the ocean, which about span the values for simple climate models found in the literature (e.g. Schlesinger and Jiang, 1990). This parameter might be used to calibrate such upwelling-diffusion energy-balance climate models to emulate AOGCM response. In Table 1 we include references and the aliases under which the various models are mentioned throughout this report. The range of IRF parameters will provide us with an estimate of the possible range of uncertainty in the dynamics of climate system response to the applied transient forcing. Note that using a model intercomparison in uncertainty assessment has two major shortcomings. First, we are unable to supply information on the *probability distribution* of the results. Second, there is no guarantee that the choice of model experiments will be complete in covering the full range of plausible outcomes.

As an example of IRF performance, Figure 2 shows results from the CSIRO GCM experiment (Watterson, 2000) and the IRF model using the appropriate parameter values. Both models were forced with the same scenario (see Table 1). For all IRF fits, we compared the Root-Mean-Square (RMS) error value of the fit to the standard deviation, if available, of global mean surface-air temperature in the control run of the AOGCMs (using constant present-day or pre-industrial greenhouse gas concentrations). The latter is a measure of natural variability, which is not captured by the IRFs, as can also be seen in Figure 2. Therefore, a fit using IRFs will make a RMS error at least as large as the standard deviation of the control run. In general, the RMS error of the IRF fit did not differ significantly from the standard variation of surface-air temperature in the AOGCM control run. However, this check on RMS of the very same scenario to which the IRF model was tuned is very limited as a performance test. Because of non-linearities in the system, which are not captured by the IRF model, the values found for the IRF constants will vary when the same AOGCM is driven by a different greenhouse gas concentration scenario (see also Hasselmann et al., 1993). The IRF model tuned to one AOGCM scenario run will therefore have a larger error when both models are forced with a different scenario. As a test, we used two different stabilization runs of the GFDL AOGCM (Manabe and Stouffer, 1994; denoted by GFDL '93 in this report). Where the 2xCO<sub>2</sub> GFDL '93 run shows a weakening of the thermohaline circulation (as indeed does the majority of coupled GCMs), the 4xCO<sub>2</sub> run includes a collapse, identified as a potential "extreme event" (Stocker and Schmittner, 1997). However, the parameters found for the two GFDL '93 runs do not differ significantly (Table 1). The last problem we encountered was that when IRF parameters are diagnosed from a longer GCM run, the balance of fast and slow response terms tends to shift to longer time scales.

As our analysis spans a few centuries, we decided to take the first 500 years of the climate model experiments, or less than that if 500 years were not available (Table 1). We intend in future to apply

a simplified, computationally very efficient AOGCM (ECBilt; Opsteegh et al., 1998) to better assess the size of the errors made with this IRF approach.

To highlight the importance of the balance between fast and slow response terms, in Figure 3 we show the response of the IRFs to a sudden doubling of CO<sub>2</sub> concentration. Note that due to the scenario dependence of IRF fits mentioned above, the IRF responses to this sudden doubling of CO<sub>2</sub> resemble only the "original" climate model response to such forcing when the same, extreme, scenario was used when determining IRF parameters. The spread of IMAGE 2.1 results show that adjusting parameters in simple climate models may offer another way to mimic AOGCM response, as extensively shown in Senior and Mitchell (submitted) for example. Also indicated in Figure 3 is

*Table 1 Summary of climate model experiments used to derive Impulse Response Functions and values of IRF parameters*

Climate model (aliases in this report)	Reference	Short description of model experiment	Climate sensitivity (°C) <sup>(3)</sup>	$\tau_1$ (yr)	$l_1$	$\tau_2$ (yr)
ECHAM1/LSG <sup>(1)</sup>	Hasselmann et al. (1993)	Instantaneous CO <sub>2</sub> doubling <sup>(2)</sup>	1.58	2.86	0.685	41.67
ECHAM3/LSG	Voss et al. (1998)	500 years used ; 1% per year CO <sub>2</sub> increase till 4×CO <sub>2</sub> is reached, then constant; total is 850 years	2.5	14.4	0.761	393
GFDL '90 <sup>(1)</sup>	Hasselmann et al. (1993)	Instantaneous CO <sub>2</sub> doubling <sup>(2)</sup>	1.85	1.2	0.473	23.5
GFDL '93 2×	Manabe and Stouffer (1994)	1% per year CO <sub>2</sub> increase till 2×CO <sub>2</sub> , then constant; total 500 years	3.5	6.5	0.671	388
GFDL '93 4×	Manabe and Stouffer (1994)	1% per year CO <sub>2</sub> increase till 4×CO <sub>2</sub> , then constant; total 500 years	3.5	8.5	0.665	233
GFDL '97	Haywood et al. (1997)	Two-member ensemble mean GHG-only historical concentrations from 1760 till 1990, then IS92a; total 300 years	3.7	12.6	0.613	145
HadCM2	Senior and Mitchell (submitted to <i>J. Clim.</i> )	500 years used; 1% per year CO <sub>2</sub> increase till 2×CO <sub>2</sub> , then constant; total 900 years	3.0	7.4	0.527	199
CSIRO	Watterson (2000)	500 years used from historical GHG forcing till 1990, then 1%/year CO <sub>2</sub> increase till 3×CO <sub>2</sub> , then constant; total 565 years	3.6	12.7	0.605	432
IMAGE 2.1 (k=0.56 cm <sup>2</sup> /s)	This report	Instantaneous CO <sub>2</sub> doubling <sup>(2)</sup>	2.37	2.19	0.654	76
IMAGE 2.1 (k=2.3 cm <sup>2</sup> /s)	This report	Instantaneous CO <sub>2</sub> doubling <sup>(2)</sup>	2.37	1.92	0.471	105
Brazilian revised <sup>(1)</sup>	Filho and Miguez (1998)	-	3.06	20	0.634	990

<sup>(1)</sup> IRF parameters were not calculated here, but adopted from reference.

<sup>(2)</sup> In an "instantaneous CO<sub>2</sub> doubling" experiment, the atmospheric CO<sub>2</sub> concentration is doubled abruptly (2×CO<sub>2</sub>), with the climate model starting from a present-day equilibrium state. The concentration is then held fixed at 2×CO<sub>2</sub>, while the model is allowed to reach a new equilibrium.

<sup>(3)</sup> Climate sensitivity was adopted from respective reference, except for HadCM2, where climate sensitivity is averaged over 500 years (Senior and Mitchell, submitted).

the response of the IRFs used in the revised Brazilian Proposal (Filho and Miquez, 1998). The parameters used there result in an “outlier” response, especially in the longer term (see also numeric values of IRF constants in Table 1), although not as extreme as reported in an earlier assessment of ours, based on a very limited set of AOGCM results (Den Elzen et al., 1999).

### *Temperature increase attributed*

As mentioned in Section 2.2, global radiative forcing from a greenhouse gas (i.e. CO<sub>2</sub>, CH<sub>4</sub> and N<sub>2</sub>O) is the sum of radiative forcings caused by emissions of individual regions. Therefore,  $Q(t')$  in Equation (3) can be replaced by the sum over these regions,  $\sum_{r=1}^R Q_r(t')$ . Placing this summation over regions outside of the convolution integral, we can apply Equation (3) to regional forcings to obtain “regional” temperature increase. All regional representations of Equation (3) thus obtained contain the same factor of  $DT_2$ . This factor cancels out when relative contributions are calculated by dividing individual regional terms by global temperature increase, which contains the same factor. This means that when determining relative contributions using our linearised approximation of the climate system response, uncertainty in climate sensitivity does not matter any longer. As we will further illustrate in section 3.3, the relative contribution as in the Brazilian Proposal depends only on the above-mentioned balance of processes on short and long time scales, determined by the IRF time-scale parameters  $l_s$  and  $t_s$ .

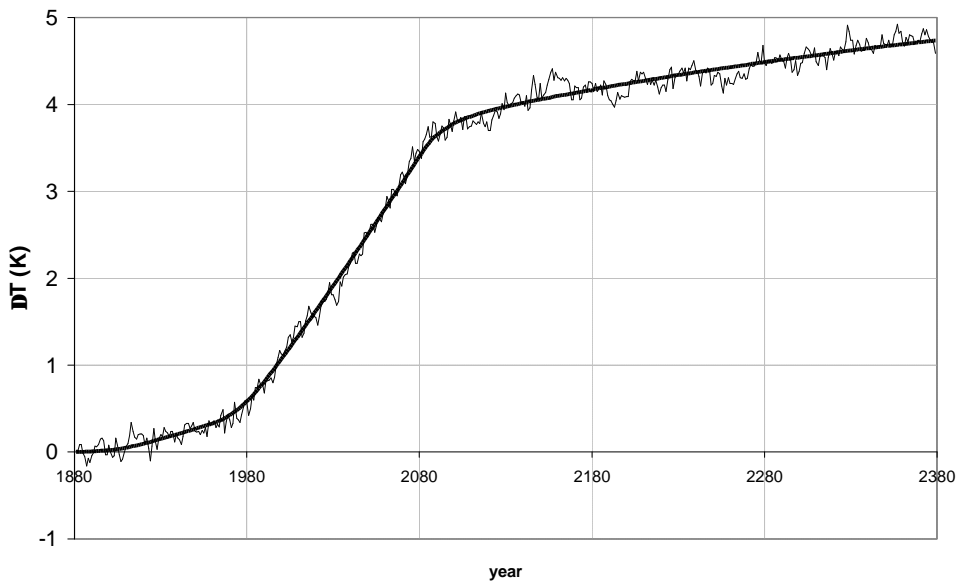


Figure 2. The IRF model (heavy line) tuned to the CSIRO GCM data (light line) (Watterson, 2000) where the radiative forcing follows the IS92a scenario, starting with the historical pathway from 1881, and stabilises at 3 × the present CO<sub>2</sub> concentration.

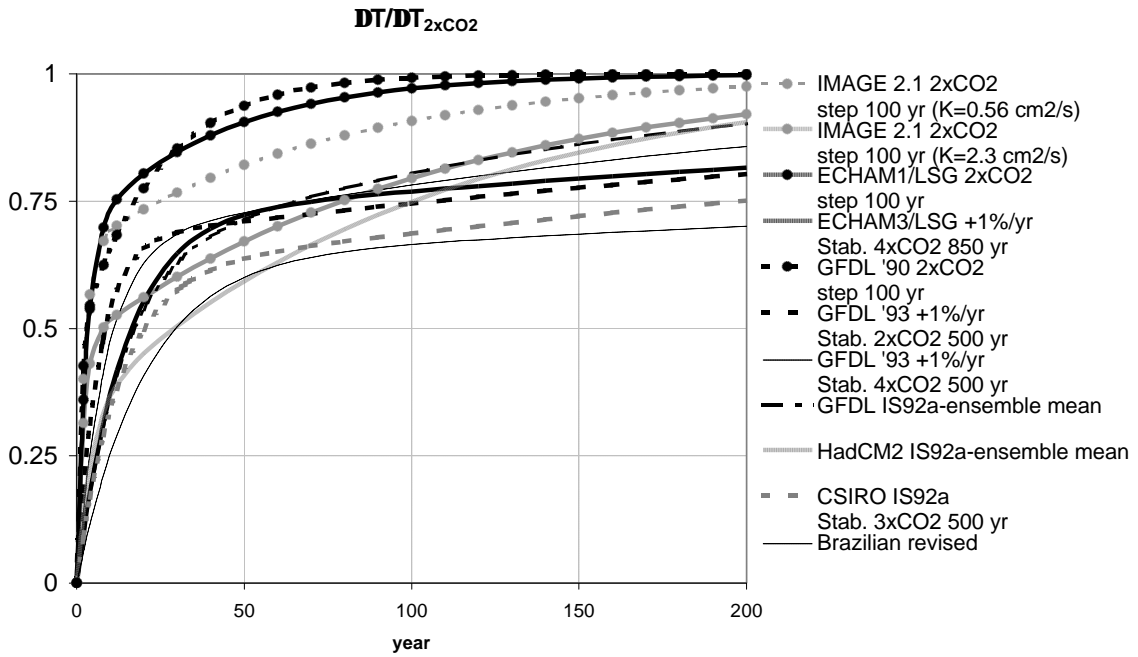


Figure 3. The temperature response (normalized by climate sensitivity) to a sudden doubling of the atmospheric  $CO_2$  concentration at time  $t=0$  for the various IRFs in Table 1.

### **3 Model analysis of a region's contribution to global warming: model uncertainties**

#### **3.1 Introduction**

In the analysis we will assess the impact of the following model uncertainties on a region's contribution to global warming: (1) various balancing procedures of the past carbon budget and other carbon cycle models; (2) various climate response functions and (3) the overall impact of these uncertainties in the global carbon and climate models.

For this analysis we use the climate assessment model as described in Chapter 2. The reference case of the calculations presented below always refers to the results of the meta-IMAGE model - the core of the climate assessment model - with its default parameter settings (Den Elzen, 1998). For this model, which starts in 1750, we assume an initial steady state before anthropogenic disturbances are imposed upon the system. The main input data of the model framework are composed of the following human-induced perturbations of the climate system: (1) anthropogenic (energy-, industrial and agriculture-related) emissions of greenhouse gases, (2) land-use changes and the associated CO<sub>2</sub> emissions. These input data will be first briefly described.

#### **3.2 Input data**

##### *Anthropogenic emissions of greenhouse gases*

The regional fossil fuel CO<sub>2</sub> emissions for the period 1751-1995 are based on the CO<sub>2</sub> emissions database of the Oak Ridge National Laboratory (ORNL), which is also referred to as ORNL-CDIAC (CO<sub>2</sub> Data and Information Assessment Center) (Marland and Rotty, 1984; Marland et al., 1999a; Andres et al., 1999). The global bunker and feedstock emissions, and the difference between the global and total sum of regional CDIAC emissions are allocated to the regional CO<sub>2</sub> emissions using the country contribution data of the EDGAR (Emission Database for Global Atmospheric Research) data set (Olivier et al., 1996; 1999); and the HYDE database (Klein-Goldewijk and Battjes, 1997) for the period 1890-1970. The ORNL-CDIAC emission data are limited to CO<sub>2</sub> emissions from fossil fuels and cement production. The historical regional anthropogenic CH<sub>4</sub> and N<sub>2</sub>O emissions (including the emissions due to land-use changes) are therefore taken from the EDGAR data set. The historical global anthropogenic emissions of the halocarbons, other greenhouse gases and ozone precursors are based on EDGAR (Olivier et al., 1999) and SO<sub>2</sub> is based on Smith et al. (2000). The regional anthropogenic CO<sub>2</sub>, CH<sub>4</sub> and N<sub>2</sub>O emissions, as well as the global emissions of the other greenhouse gases and SO<sub>2</sub> for the 1995 to 2100 period are based on the IMAGE 2.1 Baseline-A scenario (Alcamo et al., 1998). This scenario is comparable with the IPCC IS92a emissions scenario.

##### *Land-use changes and associated CO<sub>2</sub> emission*

The historical regional CO<sub>2</sub> emissions from land-use changes are based on Houghton and Hackler (1995) and Houghton et al. (1983; 1987), with a further aggregation to the 13 regions according to regional past population trends. The global CO<sub>2</sub> emissions estimate for the period 1850 to 1980 (115 GtC) and the 1980-1990 average flux (1.4 GtC·yr<sup>-1</sup>) are almost identical to the IPCC 1995 estimates (Schimel et al., 1995). A recent revised analysis of Houghton (1999) shows a somewhat higher estimate for the 1980s (2.0 GtC·yr<sup>-1</sup>), but an almost similar estimate for the 1850-1980 total flux. These revised regional emissions have not been adopted here, since we wanted to use the global carbon balance estimates of the IPCC 1995 scientific assessment (Schimel et al., 1995). The land-

use changes - important for the terrestrial carbon-cycling processes - are also based on Houghton and Hackler (1995), but further disaggregated in the four major land cover types: forests, grasslands, agriculture and other land, for the developing and industrialized world, as used in meta-IMAGE.

The area changes for the four land-use categories (forests, grasslands, agricultural and other land) in the developing and industrialized world for the period 1990-2100 are also based on aggregated land-use data of the Baseline-A scenario. The 1995-2100 regional CO<sub>2</sub> emissions from land-use changes are also based on the Baseline-A scenario.

### ***3.3 Various balancing approaches for the past carbon budget***

To investigate the sensitivity of the global CO<sub>2</sub> concentration and temperature increase, and the contribution of specific regions (i.e. the Annex I and non-Annex I regions) for balancing the past carbon budget, we performed a sensitivity analysis using the global carbon cycle model of meta-IMAGE. In the reference case, model parameters representing the key terrestrial feedbacks (i.e. the CO<sub>2</sub> fertilization effect and temperature feedback on net primary production and soil respiration) and oceanic uptakes are set on the default values used within meta-IMAGE. This leads to a balanced past carbon budget and a good fit between the historically observed and simulated CO<sub>2</sub> concentrations. The simulated carbon fluxes of the components of the carbon budget for the 1980s (1980-1989) are similar to the IPCC estimates (Table 2). The atmospheric CO<sub>2</sub> concentration projection for the IS92a emissions scenario is about 690 ppmv in 2100, which is somewhat lower than the central IPCC and MAGICC projection of approximately 705-710 ppmv (revised 1994 carbon budget) (Schimel et al., 1995). The latter is a direct result of the assumed high CO<sub>2</sub> fertilization effects and high agricultural carbon uptake within meta-IMAGE (both resulting from the consistency with IMAGE 2.1) (Den Elzen, 1998). Figures 4b&c give the projections of the CO<sub>2</sub> concentration and temperature increase for the Baseline-A scenario. The temperature increase projection uses the total radiative forcing from changes in the concentrations of all greenhouse gases and aerosols as input. The resulting temperature increase for the reference case is about 3.1 °C for the period 1750 (pre-industrial) to 2100.

In the following sensitivity experiments the scaling factors for the ocean flux, emissions from land-use changes, northern hemispheric terrestrial uptake, and CO<sub>2</sub> fertilization feedback parameters, are varied so that the set of parameter combinations will lead to a well-balanced past carbon budget. The temperature feedback parameters are kept at their default values. The simulated carbon fluxes of the carbon budget, i.e. the oceanic and terrestrial carbon uptake, and the CO<sub>2</sub> emissions from land-use changes during the 1980s, should be between the upper and lower boundaries of the IPCC estimates (Table 2). In the first two extreme "oceanic uptake" cases, a high and a low oceanic uptake, the scaling factors for the ocean flux are set at the maximum and minimum values. This results in the 1980s oceanic uptake of 3.0 and 1.0 GtC yr<sup>-1</sup>, respectively. The balanced past carbon budget is now achieved by scaling the CO<sub>2</sub> fertilization feedback parameters and the northern hemispheric terrestrial uptake. The terrestrial sink for the 1980s then varies between 0.8 and 2.3 GtC yr<sup>-1</sup> (Table 2). These two cases have been selected from other similar conditioned simulation experiments as two extreme examples of the balancing variations in the terrestrial and oceanic uptake fluxes (representing the terrestrial and oceanic uncertainties, in which the impact of variations in the temperature feedback parameters is ignored). The resulting projected CO<sub>2</sub> concentration range in 2100 varies between 687 and 719 ppmv (717 ppmv for the reference case).

The following experiments consider the uncertainties in the CO<sub>2</sub> emissions from land-use changes (land-use sources and carbon sink uncertainties) by setting its scaling factor at maximum and minimum values (emissions during the 1980s between 0.6-2.6 GtC yr<sup>-1</sup>) (Table 2). The extreme upper and lower CO<sub>2</sub> concentration projections are now achieved (662 and 794 ppmv, respectively,

by 2100), by balancing the past carbon budget with only the CO<sub>2</sub> fertilization effect, while the oceanic parameters are kept constant.

Figures 4d-f depict the Annex I and non-Annex I contributions to global anthropogenic CO<sub>2</sub> emissions, CO<sub>2</sub> concentration, and temperature increase and uncertainty ranges based on these sensitivity experiments. Taking the central reference case, the moment of convergence of Annex I and non-Annex I contributions is shown to be delayed from 2015 (anthropogenic CO<sub>2</sub> emissions) to 2045 (CO<sub>2</sub> concentration) to 2050 (temperature increase). Uncertainties in the terrestrial and oceanic uptake do not affect the contribution outcomes. However, when also the uncertainties in the CO<sub>2</sub> emissions from land-use changes are included, the convergence year of equal Annex I and non-Annex I contribution to temperature increase varies between 2030 and 2065. The uncertainty range of Annex I contribution to the 1990 temperature increase becomes 57% to 75% (65% for the reference case). Over time, the influence of the uncertainties in the land-use CO<sub>2</sub> emissions on the contribution projections decreases rather quickly, mainly due to the dominating role of fossil fuel CO<sub>2</sub> emissions in the total anthropogenic CO<sub>2</sub> emissions, but also to the decay of past (uncertain) emissions. After 2025 the uncertainties in the contribution projections become even almost negligible. The anthropogenic CO<sub>2</sub> emissions are then almost entirely (about 95%) determined by the fossil CO<sub>2</sub> emissions, which are more than double the 1995 value, whereas the land-use emissions somewhat stabilizes at about 50% of its present value (See also Figure 4a).

As mentioned in section 2.1, we have implemented an idealized form of a carbon “sink-to-source shift” of the terrestrial biosphere after 2050. The dashed line in Figure 4 clearly indicates the consequences of such a shift. However, this does not show up at all in the representation of the contributions. The increase in atmospheric CO<sub>2</sub>, as compared to a case without a “sink-to-source shift”, is not attributed to any specific region and only exerts an influence through a lengthening of atmospheric CO<sub>2</sub> lifetime. This is combined with the contribution of a region being determined by emissions in a period of more than a hundred years before an evaluation point. Therefore changes in CO<sub>2</sub> lifetime at the very end of this assessment might not have a significant effect.

We also did the experiments for the reference case implementing the IPCC Bern carbon cycle model, as described in Joos et al. (1996), and the MAGICC carbon cycle model, as described in Wigley and Raper (1992) and Wigley (1991). The first results for the Annex I and non-Annex I contributions to the temperature increase for these two cycle models show almost the same results as the meta-IMAGE model.

*Table 2 Components of the carbon budget (in GtCyr<sup>-1</sup>) based on model simulations for the carbon balancing experiments for the period 1980-1989 according to the IPCC (Schimel et al., 1995).*

Component	IPCC estimate	Reference case	High oceanic uptake	Low oceanic uptake	High deforestation	Low deforestation
CO <sub>2</sub> emissions from fossil fuel burning and cement production ( $E_{fos}$ )	$5.5 \pm 0.5$	5.5	5.5	5.5	5.5	5.5
CO <sub>2</sub> emissions from land-use changes ( $E_{land}$ )	$1.6 \pm 1.0$	1.6	1.6	1.6	2.6	0.6
Change in atmospheric CO <sub>2</sub> ( $dC_{CO_2}/dt$ )	$3.3 \pm 0.2$	3.3	3.3	3.3	3.3	3.3
Uptake by the oceans ( $S_{oc}$ )	$2.0 \pm 0.8$	2.0	3.0	1.0	2.0	2.0
Uptake by Northern Hemisphere forest regrowth ( $E_{for}$ )	$0.5 \pm 0.5$	0.5	0.0	0.5	0.5	0.5
Additional terrestrial sinks (IPCC: $[E_{fos} + E_{land}] - [dC/dt + E_{for} + S_{oc}]$ )	$1.3 \pm 1.6$	1.3	0.8	2.3	2.3	0.3

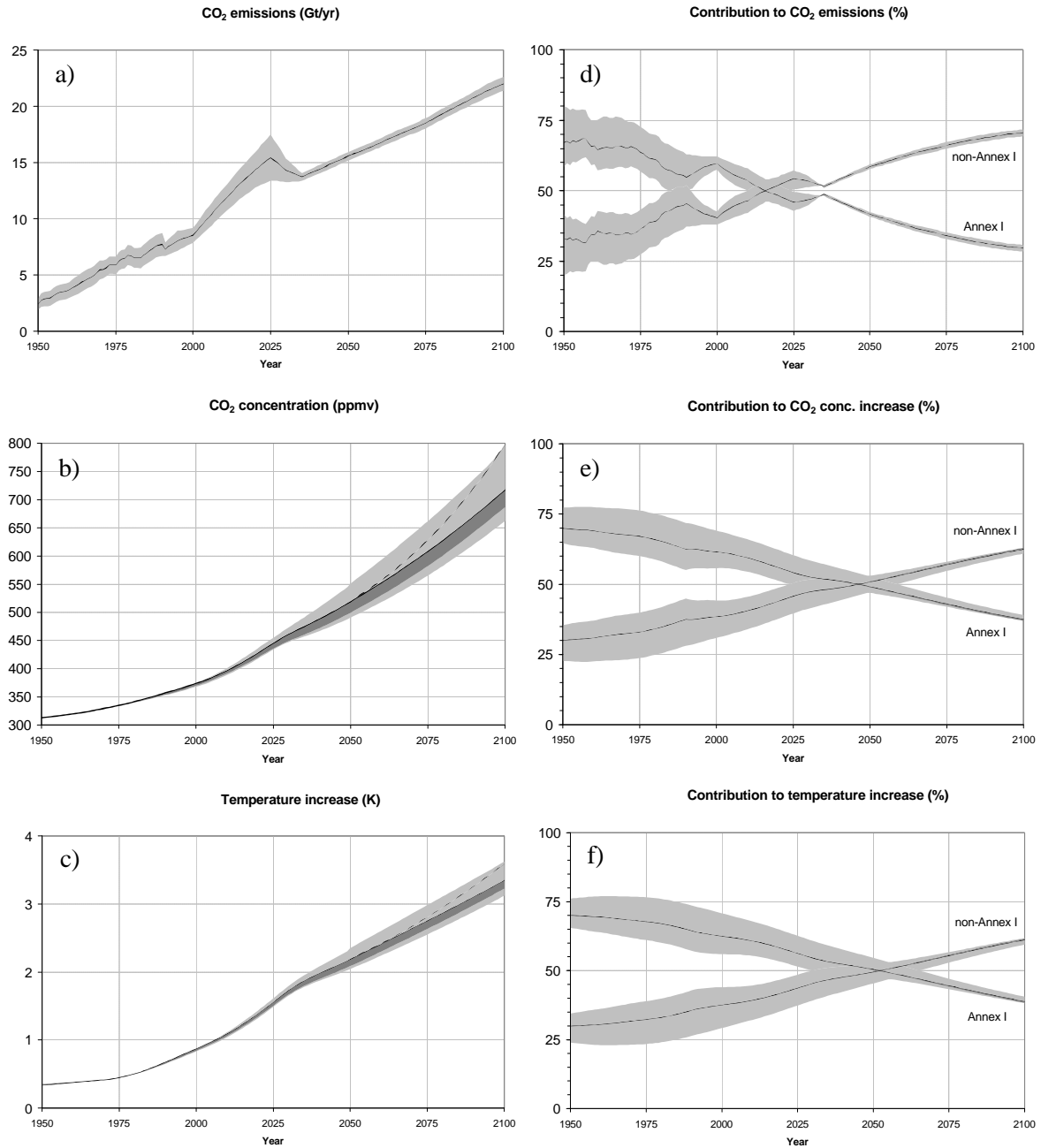


Figure 4. The global anthropogenic CO<sub>2</sub> emissions, CO<sub>2</sub> concentration and temperature increase (left column) and the contribution of Annex I and non-Annex I (right column) for the Baseline-A scenario according to the meta-IMAGE model for the carbon balancing experiments (solid line). The two uncertainty ranges represent the uncertainties in the terrestrial and oceanic carbon sink fluxes (dark-grey), and in the sink and land-use sources (light-grey). The temperature increase is calculated using as input the total radiative forcing from changes in the concentrations of all greenhouse gases and aerosols. Also indicated is the terrestrial “sink-to-source shift” case (dashed line).

### 3.4 Using temperature response functions of various AOGCMS

As explained in section 2.3, we will apply the results of a number of climate models to reflect uncertainty in climate modelling. Figure 3 has already illustrated the spectrum of response time scales diagnosed from the AOGCM experiments. Using this range of different response time scales and the differing climate sensitivities of the AOGCMs, we will show the resulting spread in projected temperature response in Figure 5a. The results of the IRF models, forced by our Baseline-A scenario, are not equal to the responses in the “original” climate model experiments, as other scenarios were used there (see Table 1). For example, our reference scenario results in  $7.4 \text{ W}\cdot\text{m}^{-2}$  radiative forcing in 2100, compared to, for example, about  $6.3 \text{ W}\cdot\text{m}^{-2}$  as given by IPCC (1995) for IS92a, or  $8.8 \text{ W}\cdot\text{m}^{-2}$  in the HadCM2 experiment (Viner, pers. comm.). Differing climate sensitivity of the models is the main factor behind the range of results in Figure 5a, as we will show later on. This also applies to rate of temperature increase as shown in Figure 5b. Models with a fast response do not necessarily show a greater rate of temperature increase, because of their relatively low climate sensitivity (compare, for example, ECHAM1/LSG or GFDL '90 in Figure 5b with Figure 3).

In Figure 6a, the solid line represents the temperature response of our meta-IMAGE reference case, which is not necessarily the most likely. In this figure, the innermost, dark-grey area depicts the range of results if all the different IRF time-scale parameters ( $t_s$  and  $l_s$  in Equation (3) and Table 1) are applied using the same IPCC “best-guess” climate sensitivity of  $2.5 \text{ }^\circ\text{C}$ . The uncertainty range broadens significantly if the IRF time-scale parameters are combined with their respective climate sensitivities in Table 1, ranging from  $1.58$  to  $3.7 \text{ }^\circ\text{C}$  (grey, compare with Figure 5a). Finally, the range broadens even further if the IRF time-scale parameters are arbitrarily combined with climate sensitivities from the full IPCC range of  $1.5 - 4.5 \text{ }^\circ\text{C}$  (light grey). Note that this exercise of combining time-scale parameters with arbitrary climate sensitivities does not necessarily result in the IRF model being able to reproduce the observed temperature increase of about  $0.6 \text{ }^\circ\text{C}$  (IPCC, 1995) up to 1990. This is directly connected to the issue of uncertainty in sulphate aerosol forcing, for which we assume central values for direct forcing only (IPCC, 1995), and natural forcings, which are not included here. Combining high climate sensitivity, resulting in a strong response to greenhouse gas concentration increases, with strong sulfate aerosol forcing might very well result in a close reproduction of the historical pathway (see, for example, Tett et al., 1999). Figure 6a clearly shows the climate sensitivity as playing a dominant role in determining the range of absolute temperature increase. However, in Figure 6b, we follow the same procedure of including more and more sources of uncertainty for relative contributions of Annex I and non-Annex I parties to temperature increase. This time, the uncertainty range expands no further than the dark-grey area, resulting from the spread in response time-scales alone. As a result, the range of Annex I contributions in 2100 is determined as comprising 39.5–42.1 percent, determined solely by the range of dynamic responses of the AOGCMs reviewed here. In our scenario, convergence of contributions of Annex I and non-Annex I is realised between 2053 and 2062. We now clearly see, as previously explained, that uncertainty in climate sensitivity plays no role when assessing relative contributions. However, we would like to stress again that the climate sensitivity remains a crucial link between emission control, and climate and other impacts.

We can also see that over time, the influence of various global temperature response functions on the contribution projections increases. Studying the contribution projections for individual regions teaches us that the influence is particularly large for countries exhibiting fast-growing emissions, i.e. China and India (non-Annex I regions). With the time delay characteristic of the climate system, the range of temperature projections is in the first order proportional to the growth rate of emissions. This will be further explained in the next section.

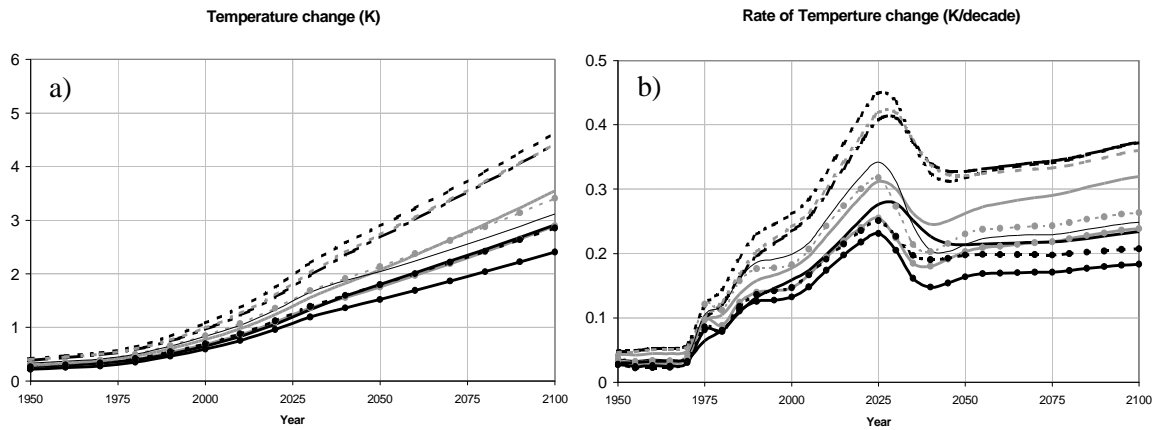


Figure 5. The temperature increase (a) and the rate of temperature increase (b) for the Baseline-A scenario using the CO<sub>2</sub> concentration pathway from the reference case according to the meta-IMAGE climate model and various IRFs of AOGCMs. The outcome of IMAGE 2.1 ( $K=2.3 \text{ cm}^2 \text{ s}^{-1}$ ), similar to ECHAM3/LSG is not shown here so as to avoid confusion. See Figure 3 for the legend.

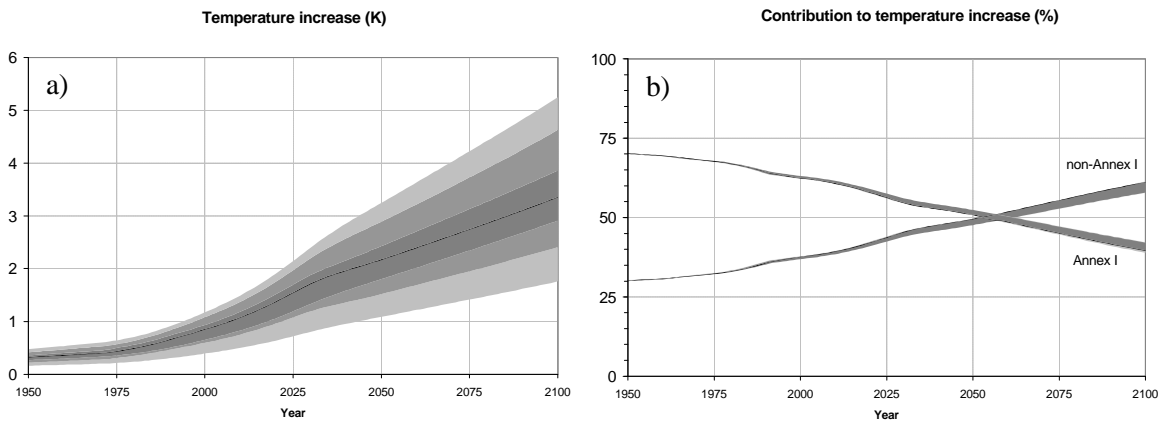


Figure 6. The temperature increase (a) and the contribution to global temperature increase of Annex I and non-Annex I (b) for the Baseline-A scenario using the CO<sub>2</sub> concentration pathway from the reference case according to the meta-IMAGE climate model (heavy line) and IRFs of AOGCMs. Dark-grey: range of outcomes for IPCC's (1995) "best-guess" climate sensitivity of 2.5 °C combined with the IRF time-scale parameters of the AOGCMs. Grey: IRF time-scale parameters combined with their respective climate sensitivities from Table 1. Light-grey: IRF time-scale parameters arbitrarily combined with climate sensitivities in the full IPCC (1995) range of 1.5 – 4.5 °C.

### 3.5 Overall uncertainties of global carbon cycle and climate models

Having analyzed the effect of some major uncertainties in the carbon cycle and climate in the preceding sections, we will now compare their relative importance for projected temperature increase. In Figure 7a, the central dark-gray area depicts total uncertainty in the carbon cycle balancing exercise (compare with Figure 4), while the gray area reflects total uncertainty from climate modeling (compare with Figure 6). The light-gray area shows the resulting total range in outcomes using the overall uncertainties in the carbon cycle and climate. The extension of uncertainty on the upper side is worth noting; this is a result of the strong temperature feedback on soil respiration as it is triggered by a high temperature increase in meta-IMAGE when a high climate sensitivity is applied.

Clearly, uncertainty in climate modeling is dominant in determining absolute temperature increase. Again, this is caused by uncertainty in climate sensitivity. The overall uncertainty in the contributions is dominated by the carbon-cycle balancing exercise i.e. the uncertainty in the land-use CO<sub>2</sub> emissions, while climate modeling only starts to make a significant addition in the course of the 21<sup>st</sup> century. Annex I contribution in 2100 is projected for this scenario as 38.8-45.0 percent. Convergence of contributions of Annex I and non-Annex I is now reached somewhere in the period of 2030-2080, compared to 2030-2065 for only carbon cycle uncertainty and 2053-2062 for climate modeling uncertainty. A combination of uncertainties and associated feedbacks extends the uncertainty range further into the future.

On a region-specific basis, we extend the analysis as shown in Figure 8. Here we have selected four regions of large historical or future emissions. Per region (USA, Western Europe, India and China), we calculated contributions to temperature increase. The extreme left-hand bars in Figures 8a-d reflect reference case values and sensitivity ranges to uncertainty in carbon cycle and climate modeling. As uncertainty is dominated by the carbon cycle until well into the next century, high historical emissions result in a high level of uncertainty. Uncertainty in climate modeling starts to play a role later on, but remains relatively minor until 2050 (see also the Appendix, Table A.1), except for regions exhibiting fast-growing emissions. For example, India where the anthropogenic CO<sub>2</sub> emissions increase more than five-fold over the period 1990-2050, the differences between a fast response IRF (like the one of ECHAM1/LSG) and a slow response IRF (CSIRO or HadCM2) leads to a absolute difference in India's contribution to global temperature increase of about 0.7% ([6.2; 6.9]%) by 2050, which is a relative difference of more than 10%. China shows in this scenario a considerable increase in its emissions for the period 2000-2020, two-fold in 20 years time. This enhanced increase in emissions leads to a contribution range for these IRFs of [10;11.3]% by 2020, thus again amounting to more than a 10% relative difference. After 2020, the increase in the emissions slows down, which decreases the differences in outcome between both IRFs (see also Figure 8).

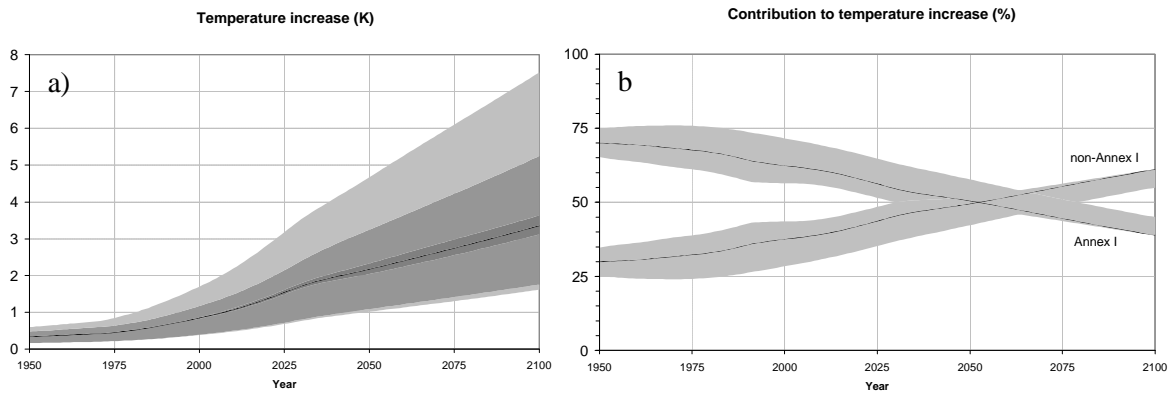


Figure 7. The global-mean surface temperature increase (a) and the contributions of Annex I and non-Annex I (b) for the Baseline-A scenario indicating the model uncertainties in the carbon cycle (dark-gray) and climate models (gray), and the combined effect of both (light-gray). For contribution, only the combined uncertainty range is shown. As a reference, the result of meta-IMAGE results is also shown here (solid line), which is not meant to represent a “best-guess” or central case.

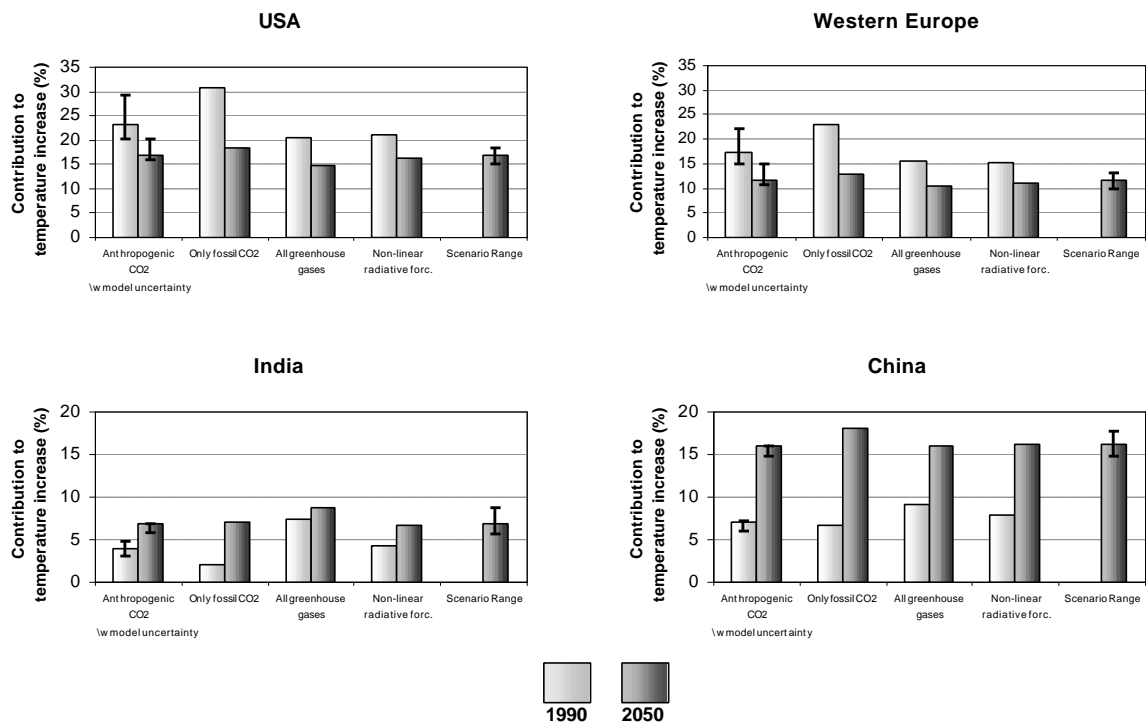


Figure 8. The contribution of the selected regions to the global-mean surface temperature increase for the Baseline-A scenario for 1990 and 2050 according to the meta-IMAGE model for the reference case (Anthropogenic CO<sub>2</sub>, including modeling uncertainty range), and 3 methodological choices (Only fossil CO<sub>2</sub>, All greenhouse gases and Non-linear radiative forcing). The right-hand column bar in each figure indicates uncertainty range for the reference case in 2050 as given by the various emission scenarios.

## 4 Model analysis of a region's contribution to global warming: methodological choices

### 4.1 Introduction

The impact of model uncertainties on calculating responsibility to climate change, attributable to specific regions, will be placed in a broader context of methodological choices by posing the following questions: (1) What is the impact of including other anthropogenic emission sources of greenhouse gases, such as methane and nitrous dioxide? (2) What is the impact of implementing the non-linear approach to calculate contributions to radiative forcing? (3) What is the impact of choosing other climate indicators, like rate of temperature change, or global-mean sea-level rise? (4) Does the impact of uncertainties and methodological choices of (1) and (2) change when the composition of the group changes within which responsibility is shared?

### 4.2 Inclusion of various anthropogenic emissions sources of greenhouse gases

In the analysis presented in the original Brazilian Proposal only the CO<sub>2</sub> emissions from fossil fuels and cement production are used to calculate country contributions to temperature increase. Omitting the CO<sub>2</sub> emissions from land-use changes evidently affects the outcomes since (a) most of the current land-use change emissions originate from developing regions, and (b) a substantial part of past emissions of more industrialized countries stem from deforestation activities. Figure 9 illustrates this effect for the Annex I and non-Annex I contributions to the temperature increase. The inclusion of these emissions seems necessary for a “proper” calculation of country contributions to global warming. The next step is to include not only the total anthropogenic CO<sub>2</sub> emissions, but also the anthropogenic emissions of non-CO<sub>2</sub> greenhouse gases like CH<sub>4</sub> and N<sub>2</sub>O. Figure 9 shows a decrease in the relative contribution of Annex I to temperature increase when taking the following (in order of appearance) into account: only fossil fuel CO<sub>2</sub> emissions, all anthropogenic CO<sub>2</sub> emissions and all anthropogenic greenhouse gases. The moment of convergence between the Annex I and non-Annex I regions shifts from 2065 for only fossil-fuel CO<sub>2</sub> emissions to 2055 for all anthropogenic CO<sub>2</sub> emissions and, finally, to 2030 for all anthropogenic greenhouse gas emissions. We can conclude that including land-use-related CO<sub>2</sub> emissions and non-CO<sub>2</sub> emissions in calculating regional contributions to temperature change sharply increases the share of non-Annex I in temperature increase. However, the uncertainty range covered by the cases “only fossil fuel CO<sub>2</sub> emissions” and “all greenhouse gas emissions” decreases in future by the increasing dominating effect of the fossil fuel CO<sub>2</sub> emissions in the overall CO<sub>2</sub>-equivalent emissions. The fossil fuel CO<sub>2</sub> emissions increase faster than the anthropogenic CH<sub>4</sub> and N<sub>2</sub>O emissions, a multiple factor (compared to 1990-emissions) of about 2.5 by 2050 compared to about 1.5-1.8, and the land-use related CO<sub>2</sub> emissions even halve compared to their 1990 levels.

A similar experiment has been done for the 13 individual regions (see also Table A.2). The results are shown for a number of selected regions in Figure 10. This picture shows a similar pattern for the Annex I and non-Annex I countries. The 1990 contribution to the global temperature increase for the United States of America and Western Europe shows a major decline when shifting from the inclusion of only the fossil CO<sub>2</sub> emissions (2nd column bars in Figures 10a-d) to the inclusion of all anthropogenic emissions of the major greenhouse gases (3rd column bars in Figures 10a-d). An opposite trend is found for the regions India and China. This trend change is somewhat decreased for the 2050 outcomes due to (1) converging levels of greenhouse gas emissions of the Annex I and non-Annex I countries (see also Figure 4) and (2) the dominating effect of the fossil CO<sub>2</sub> emissions in the overall CO<sub>2</sub>-equivalent emissions by 2050 compared to the 1990-situation.

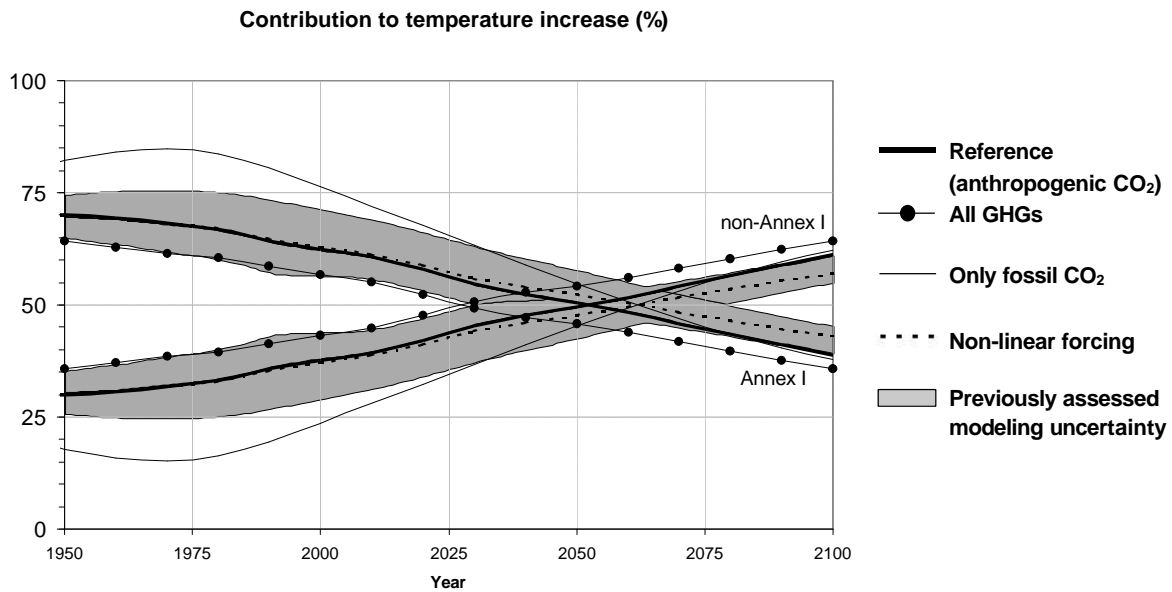


Figure 9. The contributions of Annex I and non-Annex I to global-mean surface temperature increase for the Baseline-A scenario according to the meta-IMAGE model for the cases of fossil fuel CO<sub>2</sub> emissions only, all anthropogenic CO<sub>2</sub> emissions, all anthropogenic greenhouse gas emissions. The non-linear radiative forcing attribution case is also depicted here. For reference, the previously assessed modelling uncertainty is indicated as the grey area.

#### 4.3 Non-linear approach to calculate contributions to radiative forcing

In this section we assess the impact of two choices for calculating regional contribution to global-mean radiative forcing: (i) one is according to the concentrations with equal radiative effects of the “early” and “late” emitters, and (ii) one in which changes in forcing are attributed according to the changes in attributed concentrations. The latter accounts for the saturation effect, implying a larger radiative effect of the early emissions, and a smaller radiative effect of the late emissions. Figure 9 illustrates the impact of this choice for the Annex I and non-Annex I contributions to the global temperature increase. This figure shows a small impact for the historical period due to the minor saturation effect of radiative forcing. However, including the saturation effect leads to a considerably higher Annex I contribution to global temperature increase for the next century. At present, the high anthropogenic CO<sub>2</sub> emissions of the non-Annex I region contribute less to the increase in radiative forcing per unit concentration increase. A similar pattern can be found for the individual regions (4th column bars in Figures 8a-d). Especially China’s contribution shows a decrease, whereas the USA’s contribution shows an increase.

#### 4.4 Other emissions scenarios

The analysis in this report does not assess the impact of uncertainties in historical emissions on contributions of regions to temperature increase. Former model analyses (Den Elzen et al., 1999) showed that in spite of a large uncertainty in the anthropogenic emissions, i.e. the CO<sub>2</sub> emissions from land-use changes and the emissions of CH<sub>4</sub> and N<sub>2</sub>O, particularly for the past, the contribution to present and future concentrations levels decreases in time, due to both lower activity levels and the atmospheric decay of past emissions. Moreover, these analyses clearly indicated a rather rapid decrease in the influence of uncertainties in historical emission estimates on future contributions to temperature increase. Given this finding we next analyzed the influence of different emission baselines on future contributions of regions to temperature change using the meta-IMAGE model.

The Baseline-emission scenarios, originating from the IMAGE 2.1 model, result basically from different assumptions for economic growth (moderate in A and B, high in C) and population growth (moderate in A and C, low in B) (Alcamo et al., 1996). The results are given in Table A.3 and, for our four selected regions, in the extreme right-hand column bars in Figures 8a-d. In conclusion, the different baselines for future CO<sub>2</sub> emissions will have a strong influence on a region's relative contributions to temperature change. The share of developing regions in the temperature increase will grow with high economic growth. This implies that the non-Annex I contribution will surpass the Annex I contribution to temperature change by 2045 in the high baseline (C) case, but only by 2076 in the low baseline (B) case (not shown). As can be seen in Figure 8, the uncertainty in future temperature contributions caused by varying projections of emissions (scenarios) is of the same order of magnitude as the previously assessed modeling uncertainty and the influence of methodological choices.

#### **4.5 *Other climate indicators: rate of temperature increase and sea-level rise***

In addition to temperature change, we also attempt to attribute rate of global temperature change and sea-level rise to individual nations or groups of nations. Both of these indicators represent possible indicators for potential climate impacts. Sea-level rise, which is of considerable interest to many coastal countries, is closely related to change in global temperatures. Hence, contributions of specific emitters to sea-level rise can be approximated by those to temperature increase, as shown by model analysis. Attributing changes in rates of global temperature change to specific emitters will result in considerably different outcomes than for average temperature change. Countries with fast-growing emissions contribute the most to rate of temperature increase, while countries with large historical emissions may only make a small contribution to rate of temperature increase. This pattern can be seen in the contribution of selected regions to the rate of temperature change for the IMAGE Baseline A emissions scenario (see Table A.3). The fast-growing emissions of the USA and Western Europe around 2015 result in an increase when compared to the contribution in 1990. By 2050, the contribution decreases dramatically due to the combined effect of a large atmospheric build-up of historical emissions for these regions and a relatively small increase in their emissions compared to those of the developing countries. Due to their fast-growing emissions and their relatively small atmospheric build-up of historical emissions, India's and China's contribution show an opposite trend. The nature of such changes and the implications and usefulness of the rate of temperature increase as a criterion for burden sharing needs much more careful study.

#### **4.6 *Responsibility attributed to Annex-I regions only***

In the previous sections, we compared the impact of uncertainties and methodological choices when responsibility for climate change is shared among all emitting parties. Obviously, the relative contribution of specific regions changes when a different group of regions is considered. Keeping in mind the main purpose of the original Brazilian proposal, burden-sharing among Annex-I countries, we will now assess the contribution and impact of uncertainties when responsibility is shared within the subgroup of Annex-I regions. Only contribution to temperature change in 1990 is considered, resulting from Annex-I emissions prior to 1990. Figure 10 compares contributions to "whole world" (the case in previous sections) with contributions to Annex-I temperature change for 6 Annex-I regions. For each region, uncertainty ranges resulting from modeling uncertainty and methodological choices as assessed in the previous sections are given. Because the Annex-I group is more homogeneous in terms of emission sources and historical development, the influence of methodological choices on the contribution to Annex-I temperature change is limited. Exceptions are CIS (Russian Federation and other former Soviet Union republics) and Oceania (Australia, New Zealand, Polynesian Island states). Within the Annex-I group, both CIS and Oceania exhibit a relatively large share of total CO<sub>2</sub> emissions related to land-use activities since the 1950s; this

causes the choice of “only fossil CO<sub>2</sub>” vs. “all anthropogenic CO<sub>2</sub>” to have a relatively strong influence.

The influence of the modeling uncertainty range is also considerably smaller for most regions when responsibility is shared among Annex-I regions only. The influence of climate modeling uncertainty generally increases somewhat (not shown) since the Annex-I countries exhibited a greater increase of emissions in the period preceding 1990. The greatest increase in climate modeling uncertainty is revealed in the contribution of CIS as a result of its most rapid recent increase of emissions (until 1990) compared to the other Annex-I regions. However, the influence of climate modeling uncertainty in 1990 is still small and overall uncertainty range decreases under influence of a great decrease in carbon cycle modeling uncertainty. Again CIS and Oceania form exceptions, showing an increase of uncertainty range. However, this may be overestimated because of the method used in our analysis. When adjusting the uncertain global land-use emissions during the exercise of balancing the budgets in our carbon cycle model, this is currently performed by scaling all regional emissions equally (percentagewise). Obviously, this will have a relatively strong influence on regions with relatively high land-use emissions. Therefore, CIS and Oceania are probably artificial exceptions to the general rule that modeling uncertainty range decreases when only contribution to Annex-I temperature change is considered. Later assessments, which include regional-specific uncertainty ranges for land-use emissions, should reveal to what extent this general conclusion indeed holds for specific regions.

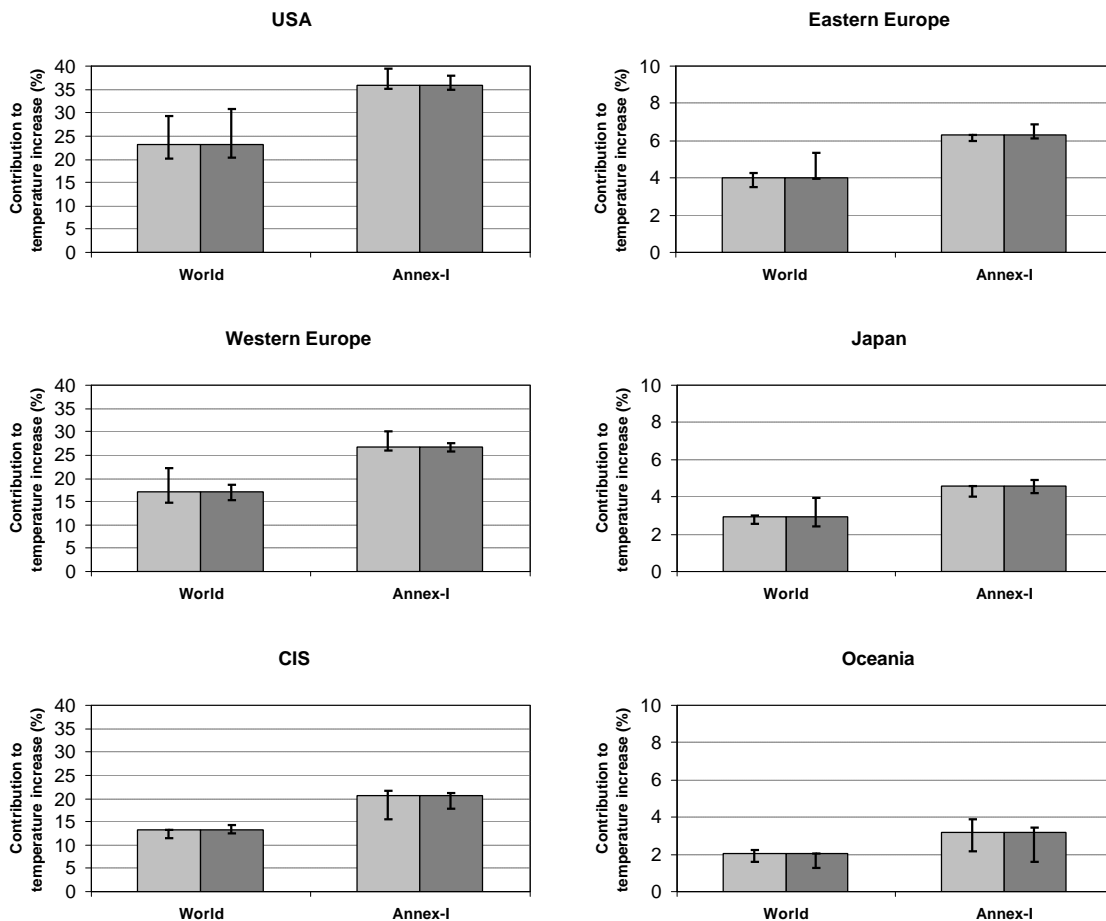


Figure 10. Contribution to temperature increase for Annex-I regions when responsibility to global temperature increase is shared among all emitting regions (“World”), or only the responsibility to the to Annex-I attributable temperature increase is shared among Annex-I regions. Note the different vertical scales in the left and right columns of this figure.

## 5 Conclusions

During the negotiations on the Kyoto Protocol, Brazil made a proposal to allocate the burden of emission reductions among the Annex I regions on the basis of the country/regional responsibility for anthropogenic climate change. Although the proposal was initially developed to help discussions on burden sharing among Annex I countries, it could also be used as a framework for discussions between Annex I and non-Annex I countries on future participation of all countries in emission reductions. By using a modeling framework, we have shown that for a central reference case the moment of convergence of contributions of Annex I and non-Annex I is delayed from 2015, for anthropogenic CO<sub>2</sub> emissions, to 2045, for CO<sub>2</sub> concentration, and, finally, to 2050 for temperature increase.

We subsequently evaluated the influence on calculating regional responsibility of (i) uncertainties in carbon-cycle and climate modeling, (ii) methodological choices, (iii) various future emission trajectories and (iv) composition of the group of regions within which relative contributions are calculated. Conclusions are presented below.

- (i) Scientific and model uncertainties largely concern the global carbon cycle and climate system dynamics, of which the influence is particularly large for countries exhibiting fast-growing emissions:
- For the carbon cycle, the uncertainties in the terrestrial and oceanic uptake do not affect the contribution outcomes. However, when the uncertainties in the CO<sub>2</sub> emissions from land-use changes are included as well, the convergence year of equal Annex I and non-Annex I contributions to global temperature increase varies between 2030 and 2065, and the uncertainty range of Annex I contribution to the 1990 temperature increase becomes 57% to 75% (65% for the reference case).
  - Over time, the influence of the uncertainties in the land-use CO<sub>2</sub> emissions on the contribution projections decreases rather quickly, mainly due to the dominating role of fossil fuel CO<sub>2</sub> emissions in the total anthropogenic CO<sub>2</sub> emissions, but also due to the decay of past (uncertain) emissions. After 2025 the uncertainties in the contribution projections become even almost negligible.
  - Using alternative carbon cycle models hardly affects the contribution projections, since the balancing procedure for these carbon cycle models with almost only CO<sub>2</sub> fertilization feedback, as prescribed by the IPCC (Enting et al., 1994), can be shown to be identical; the simulated terrestrial and oceanic carbon uptake are comparable.
  - As an example of a so-called “extreme event”, we have assessed the effect on our analysis of a shift in the role of the terrestrial biosphere in the global carbon cycle of sink to source, starting in 2050. We conclude that such extreme events will have little direct effect on calculations of regional contributions, unless the impacts are explicitly attributed to certain parties. If extreme events occur early on in the time frame of the analysis (unlike our example), further study should suggest whether they might have a significant effect by influencing, for example, atmospheric lifetimes or the dynamic response of the climate system by triggering a qualitative change of system state. As in the case of the saturation effect (see below), any rule for attributing the influence of extreme events to individual regions directly should be subject to a broad discussion.
  - Climate sensitivity plays a dominant role in determining the range of absolute temperature increase, but has no influence on the contribution projections. The influence of climate response on contributions is entirely determined by parameters characterizing the time scale of response of the climate system. In our modeling framework we see that the influence over time of various global temperature response functions on the contribution projections increases. In general, the uncertainty range of climate response widens in periods following sharp changes in radiative forcing. Studying the contribution projections of individual regions teaches us that the influence is particularly large for countries exhibiting fast-growing emissions, i.e. China and India (non-Annex I regions).
  - Altogether, uncertainty in absolute temperature increase is dominated by climate modeling, which is caused by uncertainty in climate sensitivity. The overall uncertainty in the contributions is dominated by the carbon cycle balancing exercise i.e. the uncertainty in the land-use CO<sub>2</sub> emissions,

while climate modeling only takes on an additional role in the course of the 21<sup>st</sup> century. This is due to a rapid increase of, by that time, already dominant emissions from non-Annex-I countries.

(ii) The model analysis of the methodological aspects shows that a few methodological choices will have a great impact on the outcome of the analysis to determine responsibility for temperature increase. The methodological choices are (in order of decreasing importance):

- taking into account not only the fossil fuel CO<sub>2</sub> emissions, but also all anthropogenic CO<sub>2</sub> emissions, including the CO<sub>2</sub> emissions associated with land-use changes;
- taking into account not only the major greenhouse gas CO<sub>2</sub>, but all major greenhouse gases;
- taking into account the linear or non-linear approach to calculate contributions to radiative forcing.

Including land-use related CO<sub>2</sub> emissions and non-CO<sub>2</sub> emissions in calculating regional contributions to temperature change sharply increases the share of non-Annex I in temperature increase. However, the range of outcomes covered by the cases “only fossil fuel CO<sub>2</sub> emissions” and “all greenhouse gas emissions” decreases in future, because of the increasing dominating effect of the fossil fuel CO<sub>2</sub> emissions in the overall CO<sub>2</sub>-equivalent emissions. Early in the 21<sup>st</sup> century this range in our projections is of the same order of magnitude as the scientific uncertainty range under (i).

Another methodological choice concerns the indicator for climate change. If the *rate* of temperature change is attributed to specific emitters, the result will differ significantly compared to outcomes when temperature change itself is attributed. Countries with fast-growing emissions contribute the most to rate of temperature increase, while countries with large historical emissions may only make a small contribution to rate of temperature increase. We suggest that the implications and usefulness of rate of change as a criterion for burden sharing needs more careful study.

(iii) Future contributions to temperature increase will be strongly determined by baseline emissions, especially for regions showing high growth in such scenario. Generally, in high growth scenarios the contribution of non-Annex I regions will increase quickly. Halfway through the 21<sup>st</sup> century, the range in future temperature change contributions caused by varying projections of emissions (scenarios) is of the same order of magnitude as the ranges resulting from modeling uncertainty (i) and methodological choices (ii).

(iv) Finally, the group of regions within which relative contributions to group-temperature change are calculated strongly determines the effect of uncertainties. If contributions are considered strictly within the Annex-I group, the uncertainties have a much smaller effect, compared to calculations of contributions on a world basis.

In summarizing, the analysis shows the size of the impact of all three aspects of uncertainty studied here to be comparable. Naturally, the uncertainty range spanned by emission scenarios expands with time. The impact of the scientific uncertainties will stay roughly the same as the time horizon is extended, while the importance of methodological aspects will gradually diminish. According to our present analysis, total regional uncertainties are high if contributions on a world basis are considered. However, if contributions are considered only within the Annex-I group, the total uncertainties seem surprisingly overseeable. The interesting question remaining, however, is whether all uncertainties and choices combined will prove to be “overseeable” enough to convince parties in the climate treaty to agree to a “judgement” based on a modeling framework as examined in this report.

## REFERENCES

- Alcamo, J.: 1994, 'IMAGE 2.0: integrated modeling of global climate change', *Water, Air, and Soil Pollution* **76**, (1-2).
- Alcamo, J., Kreileman, G.J.J., Bollen, J.C., Born, G.J. van den, Gerlagh, R., Krol, M.S., Toet, A.M.C. and Vries, H.J.M. de: 1996, 'Baseline scenarios of global environmental change', *Global Env. Change* **6**, (4), 261-303.
- Alcamo, J., Leemans, R. and Kreileman, G.J.J.: 1998, 'Global change scenarios of the 21st century. Results from the IMAGE 2.1 model', Elsevier Science, London.
- Andres, R.J., Fielding, D.J., Marland, G., Boden, T. A. and Kumar, N.: 1999, 'Carbon dioxide emissions from fossil fuel use, 1751-1950'. *Tellus*, in press. This data set has been integrated into CDIAC data set NDP-030 'Global, Regional, and National CO<sub>2</sub> Emission Estimates from Fossil Fuel Burning, Cement Production, and Gas Flaring, 1751-1996'.
- Berk, M.M. and Elzen M.G.J. den: 1998, 'The Brazilian Proposal evaluated', *CHANGE* **44**, 19-23.
- Berlin Mandate: 1995, <http://cop4.unfccc.de/>.
- Cess, R.D., Potter, G.L., Blanchet, J.P, Boer, G.J., Ghan, S.J., Kiehl, J.T., Le Treut, H., Li, Z.-X., Liang, X.-Z., Mitchell, J.F.B., Morcrette, J.-J., Randall, D.A., Riches, M.R., Roeckner, E., Schlesse, U., Slingo, A., Taylor, K.E., Washington, W.M., Wetherald, R.T., Yagai, I.: 1989, 'Interpretation of cloud-climate feedback as produced by 14 atmospheric general circulation models', *Science* **245**, 513-516.
- Cramer, W., Bondeau, A., Woodward, F.I., White, A. (2000): 'Global reponse of terrestrial ecosystem structure and function to CO<sub>2</sub> and climate change: results from six dynamic global vegetation models', *Global Change Biol.*, in press.
- Elzen, M.G.J. den: 1998, 'The meta-IMAGE 2.1 model: an interactive tool to assess global climate change', National Institute of Public Health and the Environment, Bilthoven, The Netherlands. RIVM report no. 461502020.
- Elzen, M.G.J. den: 1999, 'Report on the Expert Meeting on the Brazilian Proposal: scientific aspects and data availability', Center Forecasts and Climate Studies (CPTEC), Cachoeira Paulista, Brasil, May 19-20, 1999.
- Elzen, M.G.J. den, Beusen, A.H.W. and Rotmans, J.: 1997, 'An integrated modelling approach to global carbon and nitrogen cycles: Balancing their budgets', *Global Biogeochem. Cycles* **11**, (2), 191-215.
- Elzen, M.G.J. den, Berk, M. Scheaffer, M., Olivier, J., Hendriks, C. and Metz, B.: 1999, 'The Brazilian Proposal and other options for International Burden Sharing: an evaluation of methodological and policy aspects using FAIR', National Institute of Public Health and the Environment, Bilthoven, The Netherlands. RIVM report no. 728001011.
- Enting, I.G.: 1998, 'Attribution of greenhouse gas emissions, concentrations and radiative forcing', Technical Paper, 363.738740994, Aspendale, Victoria, Australia.
- Enting, I.G., Wigley, T.M.L. and Heimann, M.: 1994, 'Future emissions and concentrations of carbon dioxide', Technical Paper 0 643 05256 9, Mordialloc, Australia.
- Filho, M.L.G. and Miguez, M., 1998, 'Time dependent relationship between emissions of greenhouse gases and climate change', Ministry of Science and Technology, Brasilia, Brazil.
- Friend, A.D., Stevens, A.K., Knox, R.G., Cannell, M.G.R.: 1997, 'A process-based, terrestrial biosphere model of ecosystem dynamics (Hybrid v3.0)', *Ecol. Mod.* **95**, 249-287.
- Haan, B.J. de, Jonas, M., Klepper, O., Krabek, J., Krol, M.S., Olendrzynki, K.: 1994, 'An atmosphere-ocean model for integrated assessment of global change', *Water, Air and Soil Pollution* **76**, 283-318.
- Harvey, L.D.: 1989, 'Effect of model structure on the response of terrestrial biosphere models to CO<sub>2</sub> and temperature increases', *Global Biogeochem. Cycles* **3** (2), 137-153.
- Harvey, L.D., Gregory, G., Hoffert, M., Jain, A., Lal, M., Leemans, R., Raper, S. Wigley, T.M.L. and Wolde, J. de: 1997, 'An introduction to simple climate model used in the IPCC Second Assessment report', Cambridge University Press, Cambridge, UK.
- Hasselmann, K., Sausen, R., Maier-Reimer, E., and Voss, R.: 1993, 'On the cold start problem in transient simulations with coupled atmosphere-ocean models', *Clim. Dyn.* **9**, 53-61.

- Haywood, J. M., Stouffer, R.J., Wetherald, R.T., Manabe, S. and Ramaswamy, V.: 1997, 'Transient response of a coupled model to estimated changes in greenhouse gas and sulfate concentrations', *Geophys. Res. Lett.* **24** (11), 1335-1338.
- Hooss, G., Voss, R., Hasselmann, K., Maier-Reimer, E., Joos, F.: 1999, 'A nonlinear impulse response model of the coupled carbon cycle-ocean-atmosphere climate system', Max Planck Institute for Meteorology, Hamburg. MPI report no. 290.
- Houghton, R.A.: 1999, 'The annual net flux of carbon to the atmosphere from changes in land- Houghton, R. A. and Hackler, J.L.: 1995, Continental scale estimates of the biotic carbon flux from land cover change, Carbon Dioxide Information Analysis Center, Oak Ridge National Laboratory, Oak Ridge, Tennessee. 18501980, ORNL/CDIAC-79
- Houghton, R.A., Hobbie, J.E., Melillo, J.M., Moore, B., Peterson, III, B.J., Shaver, G.R. and Woodwell, G.M.: 1983, 'Changes in the carbon content of terrestrial biota and soils between 1860 and 1980: A net release of CO<sub>2</sub> to the atmosphere', *Ecol. Monogr.* **53**, 235-262.
- Houghton, R.A., Boone, R.D., Fruci, J.R., Hobbie, J.E., Melillo, J.M., Palm, C.A., Petersomn, B.J., Shaver, G.R., Woodwell, G.M., Moore, B., Skole, D.L. and Myers, N.: 1987, 'The flux of carbon from terrestrial ecosystems to the atmosphere in 1980 due to changes in land-use: Geographical distribution of the global flux', *Tellus, Ser. B39*, 122-139.
- IPCC: 1995, 'The science of climate change', Contribution of working group I to the second assessment report of the intergovernmental panel on climate change, Cambridge University Press, Cambridge, UK.
- Joos, F., Bruno, M., Fink, R., Siegenthaler, U., Stocker, T., Le Quere, C. and Sarmiento, J. L.: 1996, 'An efficient and accurate representation of complex and biospheric models of anthropogenic carbon uptake', *Tellus* **48B**, 397-417.
- Klein Goldewijk, C.C.M. and Battjes, J.J.: 1997, 'A Hundred Year (1890-1990) Database for Integrated Environmental Assessments (HYDE, version 1.1)', National Institute of Public Health and the Environment, Bilthoven, The Netherlands. RIVM report no. 422514 002.
- Krol, M.S. and Woerd, H. van der: 1994, 'Simplified calculation of atmospheric concentration of greenhouse gases and other constituents for evaluation of climate scenarios', *Water, Air and Soil Pollution* **76** (1-2), 259-281.
- Manabe, S. and Stouffer, R.J.: 1994, 'Multiple-century response of a coupled ocean-atmosphere model to an increase of atmospheric carbon dioxide', *J. Clim.* **7**, 5-23.
- Marland, G. and Rotty, R.M.: 1984, 'Carbon dioxide emissions from fossil fuels: a procedure for estimation and results for 1950-1982', *Tellus* **36B**, 232-261.
- Marland, G., Boden, T.A., Andres, R. J., Brenkert, A. L., and Johnston C.A.: 1999a, 'Global, regional, and national fossil fuel CO<sub>2</sub> emissions'. In: *Trends: A Compendium of Data on Global Change*, Carbon Dioxide Information Analysis Center (CDIAC), Oak Ridge National Laboratory (ORNL), Oak Ridge, Tennessee (<http://cdiac.esd.ornl.gov>).
- Marland, G., Brenkert, A. and Olivier, J.G.J.: 1999b, 'CO<sub>2</sub> from fossil fuel burning: a comparison of ORNL and EDGAR estimates of national emissions', *Env. Science & Policy* **2**, 265-274.
- Nadelhoffer, K.J., Emmett, B.A., Gundersen, P., Kjonaas, O.J., Koopmans, C.J., Schleppi, P., Tietema, A. and Wright, R.F.: 1999, 'Nitrogen deposition makes a minor contribution to carbon sequestration in temperate forests', *Nature* **398**, 145-148.
- Olivier, J.G.J., Bouwman, A.F., Van der Maas, C.W.M., Berdowski, J.J.M., Veldt, C., Bloos, J.P.J., Visschedijk, A.J.H., Zandveld, P.Y.J. and Haverlag, J.L.: 1996, 'Description of EDGAR Version 2.0: A set of global emission inventories of greenhouse gases and ozone depleting substances for all anthropogenic and most natural sources on a per country basis and on 1°x1° grid', RIVM, Bilthoven, The Netherlands. RIVM report no. 771060 002 / TNO-MEP report no. R96/119.
- Olivier, J.G.J., Bouwman, A.F., Berdowski, J.J.M., Veldt, C., Bloos, J.P.J., Visschedijk, A.J.H., Maas, C.W.M. van der and Zandveld, P.Y.J.: 1999, 'Sectoral emission inventories of greenhouse gases for 1990 on a per country basis as well as on 1°x1°', *Env. Science and Policy* **2**, 241-263.
- Opsteegh, J. D., Haarsma, R. J., Selten, F. M. and Kattenberg, A.: 1998, 'ECBILT: a dynamic alternative to mixed boundary conditions in ocean models', *Tellus* **50A**, 348-367.
- Osborn, T.J. and Wigley, T.M.L.: 1994, 'A Simple model for estimating methane concentrations and lifetime variations', *Clim. Dyn.* **9**, 181-193.
- Schimel, D., Enting, I.G., Heimann, M., Wigley, T.M.L., Raynaud, D., Alves D., and Siegenthaler, U.: 1995, 'CO<sub>2</sub> and the carbon cycle', In: *Radiative forcing of climate change and an evaluation of the IPCC IS92*

- emission scenarios*, J.T. Houghton, L.G. Meira Filho, J. Bruce, H. Lee, B.A. Callander, E. Haites, N. Harris and K. Maskell (eds.), Cambridge University Press, Cambridge, UK, pp. 35-71.
- Schlesinger, M. E., and Jiang, X.: 1990, 'Simple model representation of atmosphere-ocean GCMs and estimation of the time scale of CO<sub>2</sub>-induced climate change', *J. Clim.* **3**, 1297-1315.
- Siegenthaler, U. and Joos, F.: 1992, 'Use of a simple model for studying oceanic tracer distributions and the global carbon cycle', *Tellus* **44B**, 186-207.
- Smith, S.J., Pitcher, H. and Wigley, T.M.L. (2000): 'Global and regional anthropogenic sulfur dioxide emissions', *Global BioGeochemical Cycles*, in press.
- Solomon, A.M. and Leemans, R.: 1997, 'Boreal forest carbon stocks and wood supply: Past, present and future responses to changing climate, agriculture and species availability', *Agr. For. Met.* **84**, 137-151.
- Stocker, T.F. and Shmittner, A.: 1997, 'Influence of CO<sub>2</sub> emission rates on the stability of the thermohaline circulation', *Nature* **388**, 862-865.
- Tett, S.F.B., Stott, P.A., Allen, M.R., Ingram, W.J., Mitchell, J.F.B.: 1999, 'Causes of twentieth-century temperature change near the Earth's surface', *Nature* **399**, 569-572.
- UNFCCC: 1992, 'Convention on Climate Change', UNEP/IUC, Geneva Executive Center, Geneva.
- UNFCCC: 1997, 'Brazil; Proposed Elements of a Protocol to the United Nations Framework Convention on Climate Change, presented by Brazil in response to the Berlin Mandate, UNFCCC/AGBM/1997/MISC.1/Add.3 GE.97-, Bonn.
- UNFCCC: 1998, 'Kyoto Protocol' (<http://www.unfccc.de>).
- Voss, R., Sausen, R. and Cubasch, U.: 1998, 'Periodically synchronously coupled integrations with the atmosphere-ocean general circulation model ECHAM3/LSG', *Clim. Dyn.* **14**, 249-266.
- Watterson, I.G.: 2000, 'Interpretation of simulated global warming using a simple model', *J. Clim.* **13**, 202-215.
- White, A., Canell, M.G.R., Friend, A.D.: 1999, 'Climate change impacts on ecosystems and the terrestrial carbon sink: a new analysis.', *Global Env. Change* **9**, 21-30.
- Wigley, T.M.L.: 1991, 'A simple inverse carbon cycle model', *Global Biogeochem. Cycles* **5** (4), 373-382.
- Wigley, T.M.L.: 1993, 'Balancing the carbon budget: Implications for future carbon dioxide concentration changes', *Tellus Ser.* **45B**
- Wigley, T.M.L. and Schlesinger, M.E.: 1985, 'Analytical solution for the effect on increasing CO<sub>2</sub> on global mean temperature', *Nature* **315**, 649-652.
- Wigley, T.M.L. and Raper, S.C.B.: 1992, 'Implications for climate and sea-level of revised IPCC emissions scenarios', *Nature* **357**, 293-300.
- Wigley, T.M.L. and Raper, S.C.B.: 1993, 'Future changes in global mean temperature and sea level'. In: *Climate and sea level change: observations, projections and implications*. Warrick, R.A., Barrow, E.M. and Wigley, T.M.L. (eds.), Cambridge, Cambridge University Press.

## APPENDIX

*Table A.1* Regional contributions to the global-mean surface temperature increase for the different cases of reference case (abbreviated as: ref. case), high and low deforestation (high/low defor.), high and low climate (high/low clim.), high and low overall climate/carbon (high/low overall) for the years 1990 and 2050.

REGION	ref. case	high defor.	low defor.	high clim.	low clim.	high overall	low overall	ref. case	high defor.	low defor.	high clim.	low clim.	high overall	low overall
	1990	1990	1990	1990	1990	1990	1990	2050	2050	2050	2050	2050	2050	2050
Canada	1.72	1.51	1.98	1.75	1.72	1.97	1.54	1.59	1.62	1.59	1.63	1.59	1.67	1.63
USA	23.31	19.78	27.98	23.97	23.06	29.18	20.10	16.95	15.88	18.60	17.94	17.06	20.34	16.10
Latin America	11.93	14.83	8.21	11.92	11.87	8.85	14.73	6.45	6.88	5.66	6.97	6.55	6.07	7.13
Africa	4.85	5.96	3.54	4.75	4.95	3.60	5.99	10.15	12.76	6.97	9.63	9.84	6.46	12.18
Western Europe	17.33	14.67	20.95	17.84	17.07	22.11	14.82	11.62	10.71	13.01	12.43	11.73	14.45	10.92
Eastern Europe	4.00	3.53	4.64	3.91	4.03	4.42	3.51	4.46	4.25	4.75	4.37	4.44	4.68	4.21
CIS	13.02	12.80	13.13	12.47	13.08	11.52	12.43	10.89	10.45	11.45	10.95	10.91	11.35	10.49
Middle East	2.10	2.18	1.93	2.05	2.14	1.70	2.17	4.72	4.61	4.83	4.36	4.72	4.32	4.57
India	4.05	4.73	2.97	4.20	4.07	3.13	4.85	6.81	6.96	6.54	6.37	6.85	5.92	6.97
China	7.00	7.26	6.56	6.79	7.14	5.98	7.19	16.08	15.63	16.46	14.98	15.98	14.89	15.42
South-East Asia	5.72	7.85	3.17	5.52	5.93	2.99	7.90	5.30	5.51	4.88	5.31	5.33	4.62	5.60
Oceania	2.05	2.29	1.63	2.07	1.98	1.59	2.21	1.28	1.24	1.28	1.41	1.30	1.35	1.29
Japan	2.91	2.62	3.32	2.76	2.95	2.98	2.57	3.71	3.51	3.98	3.66	3.70	3.89	3.48
Annex I	64.3	57.2	73.6	64.8	63.9	73.8	57.2	50.5	47.7	54.7	52.4	50.7	57.7	48.1
Non-Annex I	35.7	42.8	26.4	35.2	36.1	26.2	42.8	49.5	52.3	45.3	47.6	49.3	42.3	51.9

*Table A.2* Regional contributions to the global-mean surface temperature increase for the different cases of only fossil fuel CO<sub>2</sub> emissions (abbreviated as: fos. CO<sub>2</sub>), all anthropogenic CO<sub>2</sub> emissions (ant. CO<sub>2</sub>) and all anthropogenic greenhouse gas emissions (all ghg), and the non-linear forcing case (non-lin. forc.) for the years 1990, 2010 and 2050 for the Baseline-A scenario.

REGION	fos. CO <sub>2</sub>	ant. CO <sub>2</sub>	all ghg	non-lin. forc.	fos. CO <sub>2</sub>	ant. CO <sub>2</sub>	all ghg	non-lin. forc.	fos. CO <sub>2</sub>	ant. CO <sub>2</sub>	all ghg	non-lin. forc.
	1990	1990	1990	1990	2015	2015	2015	2015	2050	2050	2050	2050
Canada	2.17	1.72	1.55	1.73	2.08	1.86	1.68	1.85	1.51	1.59	1.43	1.63
USA	30.71	23.12	20.48	23.77	25.80	21.28	18.68	21.83	18.41	16.90	14.89	17.96
Latin America	4.87	11.89	11.34	12.06	4.33	8.10	8.90	8.63	4.88	6.42	7.27	7.00
Africa	2.52	4.88	5.63	4.81	2.95	7.81	8.69	7.39	5.14	10.16	11.26	9.71
Western Europe	22.95	17.17	15.59	17.71	18.19	14.95	13.37	15.49	12.76	11.58	10.38	12.44
Eastern Europe	5.34	4.03	4.03	3.93	4.98	4.11	3.94	4.06	5.01	4.46	4.17	4.37
CIS	14.28	13.18	12.46	12.59	12.58	11.30	11.05	11.23	11.76	10.89	10.54	10.88
Middle East	1.97	2.13	2.28	2.04	3.48	3.11	3.58	2.94	5.36	4.74	5.27	4.34
India	1.99	4.02	7.36	4.11	3.55	4.29	6.79	4.29	7.14	6.83	8.73	6.36
China	6.74	7.08	9.18	6.83	12.42	11.68	12.42	11.03	18.14	16.13	16.11	14.98
South-East Asia	1.26	5.80	5.63	5.54	3.40	5.62	5.70	5.53	4.61	5.30	5.57	5.28
Oceania	1.26	2.04	2.02	2.06	1.47	1.94	1.95	1.96	1.20	1.28	1.29	1.40
Japan	3.93	2.95	2.45	2.81	4.76	3.95	3.24	3.76	4.10	3.71	3.08	3.66
Annex I	80.6	64.2	58.6	64.6	69.9	59.4	53.9	60.2	54.7	50.4	45.8	52.3
Non-Annex I	19.4	35.8	41.4	35.4	30.1	40.6	46.1	39.8	45.3	49.6	54.2	47.7

*Table A.3* Regional contributions to the rate of temperature increase for the years 1990, 2010 and 2050 for the IMAGE Baseline-A scenario (only anthropogenic CO<sub>2</sub> emissions) (first three columns), and to the global-mean surface for various IMAGE Baseline scenarios A, B and C (abbreviated as: Bas A/B/C).

REGION	Rate of temperature increase			Bas A	Bas B	Bas C
	1990	2015	2050	2050	2050	2050
Canada	1.44	1.47	0.59	1.59	1.80	1.39
USA	13.11	14.90	3.61	16.90	18.38	15.15
Latin America	10.88	0.00	5.19	6.42	7.16	5.29
Africa	8.57	15.23	8.52	10.16	8.49	10.58
Western Europe	7.29	9.24	1.29	11.58	13.13	10.16
Eastern Europe	4.98	5.71	4.13	4.46	4.52	4.77
CIS	16.70	11.46	9.56	10.89	11.14	11.59
Middle East	3.42	4.78	8.00	4.74	3.98	4.40
India	4.02	7.58	21.61	6.83	5.66	8.74
China	12.53	19.98	27.85	16.13	14.83	17.79
South-East Asia	12.06	4.15	7.26	5.30	5.40	5.47
Oceania	0.14	0.90	-0.07	1.28	1.51	1.13
Japan	4.85	4.61	2.47	3.71	3.98	3.55
Annex I	48.5	48.3	21.6	50.4	54.5	47.7
Non-Annex I	51.5	51.7	78.4	49.6	45.5	52.3